TEARHS - Modelling toxic impacts on the airway system from exposure to fluctuating concentrations

Duijm, N.J.; Markert, Frank; Ott, Søren

Publication date:
2000

Document Version
Publisher's PDF, also known as Version of record

Risø-R-1208(EN)

TEARHS - Modelling Toxic Impacts on the Airway System from Exposure to Fluctuating Concentrations

Nijs Jan Duijm, Frank Markert, Søren Ott

Risø National Laboratory, Roskilde
August 2000

Abstract. This report describes Risøs contribution to the TEARHS project. The aim of the TEAHRS project is to develop and assess methodologies to determine the acute toxicity of inhalation of fluctuating concentrations of hazardous substances as a contribution to the improvement of quantitative risk assessment.

A mathematical model is described that predicts the physical and chemical processes in the airways during short exposures to toxic substances. Based on this modelling, it has been assessed how fast and to what level tissue in the airways is exposed to the substance. These time scales turn out to be small, in the order of a few seconds. Considering the aspiration pattern, it is concluded that relevant time scale for absorption in the airways is 5 to 10 seconds. In real atmospheric, toxic gas clouds, fluctuations at this time scale are large. There is still a large gap between the empirical information on toxic effects and the relevant time scale for exposure. Concentration-time-fatality relations are obtained from experiments with rats down to 5 minutes of exposure. If the information from these relations is extrapolated down to 5 to 10 seconds using different assumptions, the predicted mortality is quite different.

This study indicates that atmospheric dispersion models for acutely toxic substances need to provide information about concentration fluctuations of time scales of 5 to 10 sec. Final conclusions can only be drawn when it becomes clear how the gap between concentration-time-fatality relations and short duration fluctuations can be closed.

ISBN 87-550-2750-4
ISBN 87-550-2751-2 (Internet)
ISSN 0106-2840

Information Service Department, Risø, 2000

Contents

Preface

This report describes the contribution of Risø National Laboratory to the project "Toxic Effects from Accidental Releases of Hazardous Substances - TEAHRS" during 1998 to 2000.

The aim of the TEAHRS project is to develop and assess methodologies to determine the acute toxicity of inhalation of fluctuating concentrations of hazardous substances as a contribution to the improvement of quantitative risk assessment.

The contribution of Risø focussed on the development of mathematical models describing the physical and chemical processes relevant for short exposures to toxic substances. The aim of this modelling is to be able to estimate how fast toxic substances penetrate into different parts of the lung. Moreover, Risø demonstrated the implications of the findings of this study using real observed exposure patterns in toxic clouds.

The activities have been organised in work packages. The work packages described in this report are:

- *Work package 3, modelling physical and chemical processes.* The largest part of this report is directly linked to this activity, which comprises the development and evaluation of a model describing the time-dependent distribution of toxic material in the body following exposure (chapters 1 to 5) and description of the hydrolysis of phosgene (chapter 9).
- *Work package 5, development of concentration-time-effect relationships*. In chapter 6, the above mentioned model has been applied to selected substances and time scales for reaching final doses in different parts of the body (internal doses), for humans as well as for rats (laboratory animals), are determined.
- *Work package 6, develop guidelines for relevant time scales in risk assessments.*
  In chapters 7 and 8, methodologies are presented and demonstrated (using real observed exposure patterns) how to use the information obtained from the time scales for internal doses in combination with the information on concentration-time-effect relationships obtained by TNO-Toxicology in the framework of TEARHS.
- *Workpackage 7, documentation.* This report documents the modelling of the physical/chemical processes, including the evaluation of these models using experimental data and other information. It is attempted to describe the models in detail, as to give the reader the possibility to judge the scientific basis of the model, including assumptions, simplifications and values of parameters. The model describing the internal dose is implemented as a Pascal code (Delphi® 3) for scientific use.

1 Morphology of the human airway system

1.1 Description and dimensions of the human airway system

Figure 1 shows the main anatomical parts of the human airway system. The parts of the system including the nose, mouth, pharynx and larynx are called the extrathoracic region, the remaining parts of the lung, from the trachea downward is the thoracic region. The thoracic region is divided in the bronchial region (trachea, main bronchi and bronchi), the bronchiolar region (bronchioles) and the alveolar region (terminal bronchioles, alveolar ducts and alveoli). The alveoli are the terminations of the airway system. They are tiny volumes (typical diameter 100-300 μm, Weibel, 1963) separated from each other by thin tissue (the interalveolar septum) of about 5-10 μm thickness, containing small capillaries to enable transfer of gas between the blood and the air in the alveoli (Weibel and Gill, 1977, Nunn, 1993).

In order to apply a simple description to reproduce air flow and diffusion in the whole airway system, we choose a regular branching model for the human airways, comparable to Weibel's "model A" (Weibel, 1963). "Regular" means that any element of the airway system is supposed to branch in 2 or more equal lower elements, as opposed to asymmetrical models, where the more general assumption is used that the lower level branches are not necessarily of equal size. Weibel's model A is also dichotomous (i.e., the elements are supposed to have 2 branches). The anticipated airflow and diffusion modelling approach does not require that the branching is dichotomous.

The basis for the airway morphology is the description as applied by the International Committee on Radiation Protection (ICRP) (ICRP, 1994). The model is based on a review of research on dimensions and geometry of the human airways. The ICRP recognises that there are significant differences in reported airway dimensions, therefore all data was scaled to a standard functional residual capacity (FRC) of 3.3 litre. The ICRP-model is the recommended model for radio-dosimetry and as such reflects considerable consensus.

The ICRP-model for the upper airways (trachea to terminal bronchioles) is based on Weibel's Model A, although the terminal bronchiole in ICRP's model is at generation 15 instead of 16 (the trachea is generation number 0). For the alveolar region, the ICRP uses a more realistic model, accounting for the fact that the individual pathways in the lung can end between the 15^{th} and 30^{th} generation. The ICRP-model accounts for 26 generations, but the number of elements of the 25^{th} and 26^{th} generation is less than the number of lower generation elements. In order to maintain a regular and almost dichotomous branching, we have joined the last three generations in one group, see Figure 1.2. In our description of the alveolar region, the average number of branches per alveolar duct varies between 2.4 (generation 20) and 1.5 (generations 23 and 24, see Table 1.1). For the dimensions (diameter and length) of bronchi and bronchioles the data from the ICRP model have been applied. Dimensions for the nasal passages have been adopted from Guilmette, Wicks and Wolff (1989). Dimensions for pharynx and larynx have been derived from Nunn (1993). The resulting branching model is included in Table 1.1. The fraction of surface covered by alveoli of the respiratory bronchioles and the number of alveoli per bronchiole is in accordance with Weibel (1963). The number of alveoli per alveolar duct is chosen in order to arrive at the total number of alveoli of 300 million.

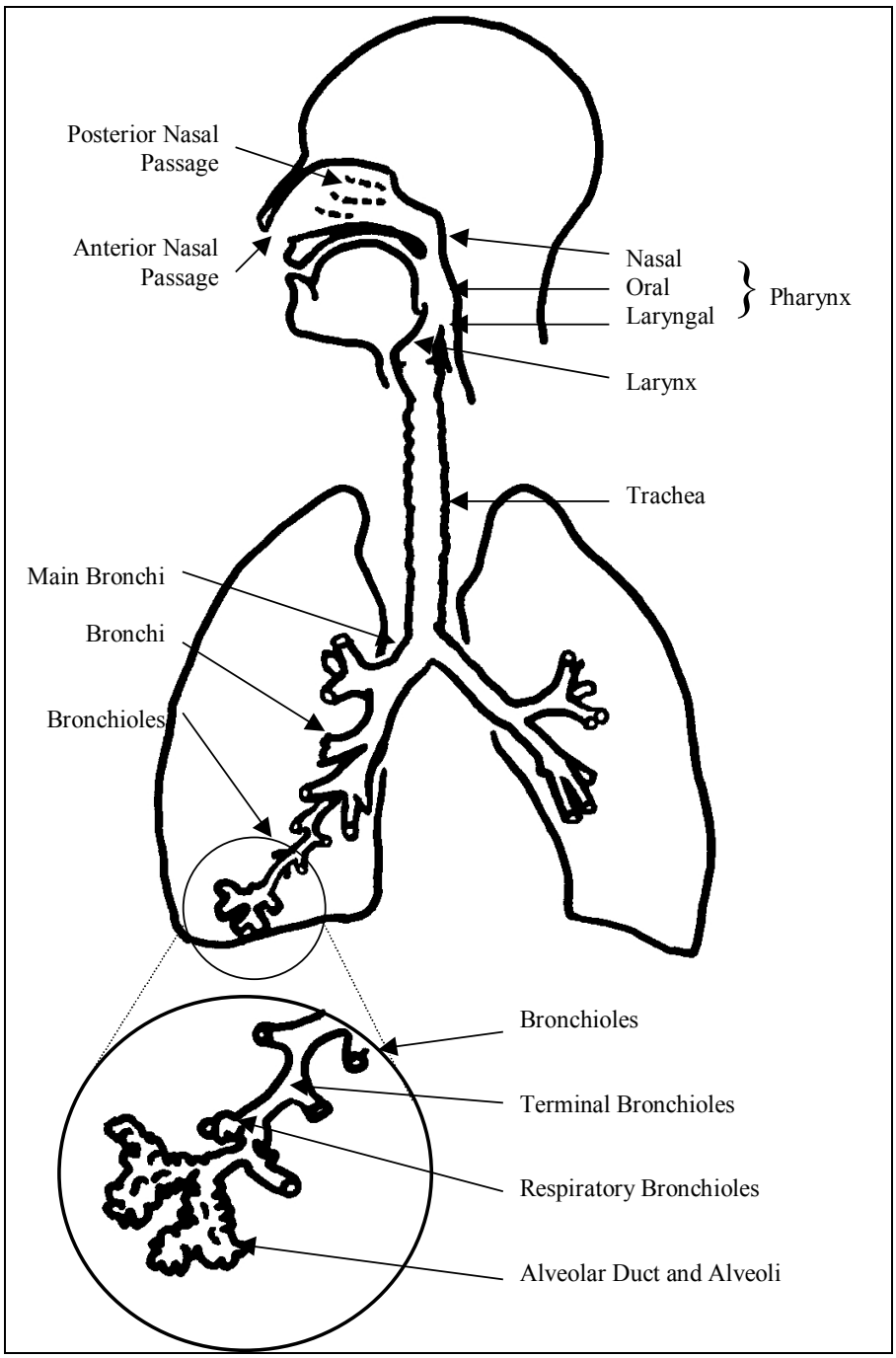

Figure 1.1. Anatomical elements of the human airways, adapted from ICRP, 1993.

Some of the total volumes and surfaces of airway regions used in the ICRP model are inconsistent with volumes and surfaces calculated using simple geometrical relations and the diameters and length of the elements as mentioned in Table 1.1. In our model the volumes and surfaces consistent with the values in Table 1.1 will be used, except for the alveoli and the upper airways above the trachea. For the alveoli independent values for surface and volume will be used as to reproduce the total sum of volumes and surfaces of the alveoli according to the ICRP. Alveolar volume and surface is 4.5 l and 140 m^2, respectively (see also Table 1.3). For the complexly shaped upper airways, volumes and surfaces are separately mentioned in Table 1.2.

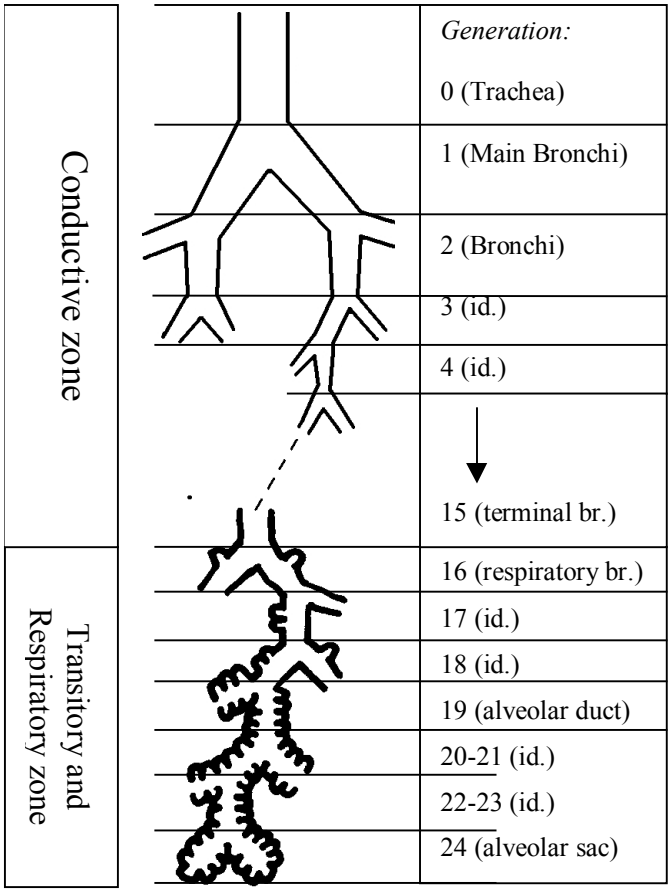

Figure 1.2. Diagram of the branching model for the human airway system, adapted from Weibel, 1963.

1.2 Airway volumes and respiration

In Table 1.1 all dimensions have been transformed to a Functional Reference Capacity (FRC) of 3.3 l. The FRC is the volume at the end of the normal expiration, with relaxed expiratory and inspiratory muscles. In this position, elastic forces from the rib cage and the diaphragm prevent complete collapse of the lung (due to surface tension in the alveoli). This means that at FRC a pressure difference of about 0.5 kPa exist between the alveoli and the pleural cavity around the lung (the transmural pressure gradient). During respiration the transmural pressure gradient can be increased to about 2 kPa. At that pressure gradient the Total Lung Capacity (TLC) is obtained. The TLC is about 3 l larger than the FRC (Nunn, 1993). One should note that FRC and TLC depend on a number of factors, like body size, sex, age, posture and lung disease (Nunn, 1993). The ICRP (1994) has published recommended scaling factors for body height, age, and sex.

Table 1.1. Regular branching human airway morphology with dimensions for a male with a Functional Reference Capacity (FRC) of 3.3 litre (scaled to FRC)

	Generation	Total number	Number of branches	Diameter at entrance (mm)	Length (mm)	Fraction of surface alveolated	Number of alveoles per duct	Total number of alveoles per generation
Mouth	-6	1	1	15.4	83.0			
Nares-nasal valve	-8	2	1	11.8	30.0			
Nasal cavity	-7	2	0.5	12.7	63.0			
Nasopharynx	-6	1	1	13.1	63.0			
Oral pharynx	-5	1	1	10.2	44.0			
Laryngal pharynx	-4	1	1	10.7	35.0			
Vestibulum laryngis	-3	1	1	16.0	20.0			
Rima glottidis	-2	1	1	7.0	2.0			
Cavum laryngis	-1	1	1	11.6	20.0			
Trachea	0	1	2	16.4	90.5			
Main bronchi	1	2	2	11.9	37.6			
Bronchi	2	4	2	8.4	14.8			
Bronchi	3	8	2	6.0	8.1			
Bronchi	4	16	2	4.3	8.8			
Bronchi	5	32	2	3.5	7.8			
Bronchi	6	64	2	2.8	6.3			
Bronchi	7	128	2	2.3	5.7			
Bronchi	8	256	2	1.9	5.0			
Bronchioles	9	512	2	1.6	4.1			
Bronchioles	10	1024	2	1.3	3.4			
Bronchioles	11	2048	2	1.0	2.8			
Bronchioles	12	4096	2	0.82	2.3			
Bronchioles	13	8192	2	0.66	1.9			
Bronchioles	14	16384	2	0.55	1.6			
Terminal bronchioles	15	32768	2	0.48	1.3	0	0	0
Respiratory bronch.	16	65536	2	0.46	0.99	0.12	6	393216
Respiratory bronch.	17	131072	2	0.41	0.82	0.25	9	1.2E+06
Respiratory bronch.	18	262144	2.25	0.36	0.67	0.5	12	3.1E+06
Alveolar duct	19	589824	2.37	0.33	0.56	1	19	1.1E+07
Alveolar duct	20	1.4E+06	2.40	0.31	0.46	1	15	2.1E+07
Alveolar duct	21	3.4E+06	2.35	0.29	0.38	1	12	4.0E+07
Alveolar duct	22	7.9E+06	1.47	0.27	0.32	1	9	7.1E+07
Alveolar duct	23	1.2E+07	1.52	0.26	0.26	1	7	8.1E+07
Alveolar sac	24	1.8E+07	0	0.26	0.18	1	4	7.1E+07
Alveoli	from 16-24			0.24	0.18			3.0E+08

By using the expiratory muscles, one can reduce the volume of the lungs below the FRC. The extra expiratory volume is the Expiratory Reserve Volume (ERV). As the lung volume decrease, in some parts of the lungs the alveoli will close, preventing ventilation and gas exchange in those parts. This volume is called the Closing Capacity (CC). The CC increases with age and it equals the FRC in upright position at about 66 years and in supine position (when the FRC is about 30% lower than in upright position) at about 44 years.

Figure 1.3 shows a normal respiration pattern with a tidal volume (V_T) of about 640 ml during 15 sec. (12 breaths per minute), followed by maximal inspiration and expiration and returning to normal breathing again.

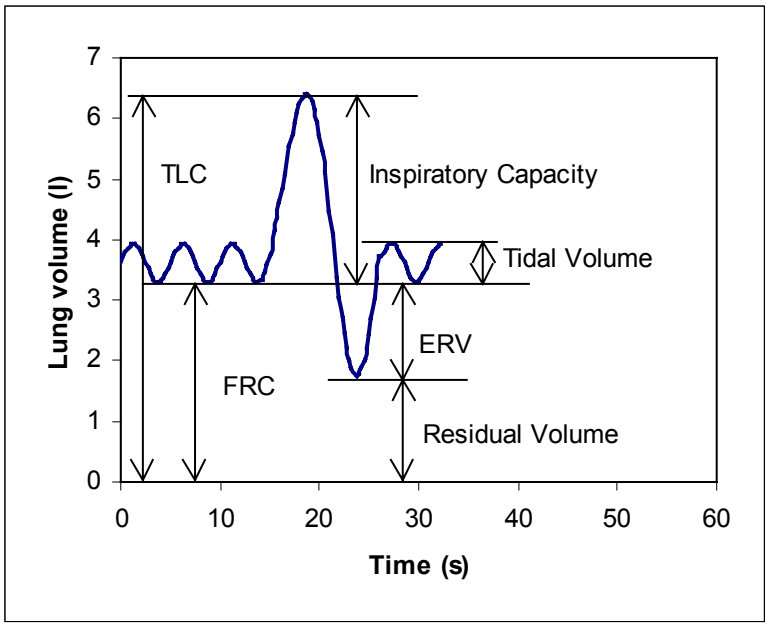

Figure 1.3. Patterns and volumes of respiration.

Table 1.2. Volumes and wall surfaces for the upper airway elements, from Guilmette, Wicks and Wolff (1989) and Nunn (1993).

	Generation	Volume (ml)	Surface (mm^2)
Mouth	-6	14.6	5896
Nares-nasal valve (both sides)	-8	6.5	5878
Nasal cavity (both sides)	-7	16.0	16300
Nasopharynx	-6	20.4	3660
Oral pharynx	-5	3.4	1404
Laryngal pharynx	-4	3.1	1200
Vestibulum laryngis	-3	4.0	1027
Rima glottidis	-2	0.07	44
Cavum laryngis	-1	2.1	726

The inflation of the lung, and thus the volume of the airway system, depends on the transmural pressure gradient. The elasticity of different lung elements is different, and the relative change in volume of the different elements is therefore also different. For a single element the volume is approximately proportional to the cube root of the transmural pressure gradient (Thorpe and Bates, 1997, for a discussion of the dynamic effect of the surface tension of the alveolar lining see Nunn, 1993). There is uncertainty with respect to the relation between alveolar surface and alveolar volume. With alveolar surface proportional to alveolar volume to a power k, i.e. $S \propto V^k$, k is reported to vary between 0.41 to 0.77 (Hoppin and Hildebrandt, 1977). In this study, we will assume geometric isotropy, i.e. k is 2/3.

Thorpe and Bates (1997) concluded that for a dog lung (Horsfield, Kemp and Phillips, 1982) the effect of transmural pressure-gradient changes on overall linear dimensions (radius and length) of airway elements can be written as:

$$\frac{x(P)}{x_{TLC}} = \alpha_k + (1-\alpha_k)\left(\frac{P}{P_{TLC}}\right)^{1/3} \qquad \textit{Equation 1.1}$$

Here α_k is the relative dimension at zero transmural pressure gradient, x(P) and x_{TLC} are the linear dimensions at transmural pressure gradient P and at TLC, respectively, and P_{TLC} is the transmural pressure gradient at TLC. Thorpe and Bates suggest a linear relation between α_k and generation number k:

$$\alpha_k = \alpha_0 - \alpha_1 \cdot k \qquad \textit{Equation 1.2}$$

Here α_0 is the relative linear dimension of the trachea (generation 0) at zero transmural pressure gradient and α_1 is a linear coefficient. Thorpe and Bates (1997) use $\alpha_0 = 0.717$ and $\alpha_{k,max} = 0.2$ for the trachea and the highest generation, respectively, in case of a dog lung. We expect that the extrathoracic elements don't inflate. We have chosen that for the human trachea $\alpha_0 = 0.9726$ and $\alpha_1 = 0{,}0274$, applying the linear relation only for $0 \leq k \leq 19$. This means that all fully alveolated alveolar ducts (generations 19 to 24 including the alveoli) are assumed to inflate with $\alpha_k = 0.452$. With this number an FRC of 3.3 l at a transmural pressure gradient of 0.5 kPa and a TLC of 6.4 l at a pressure gradient of 2 kPa is reproduced. It is noted that the compliance of the trachea, bronchi and bronchioles has an almost negligible effect on the FRC and TLC due to the limited volume involved.

Equation 1.1 suggests that there is a one to one relation between pressure and geometry (length, area and volume). This relation neglects the hysteresis that appears in the lung (Nunn, 1993). Due to hysteresis, the transmural pressure gradient during inflation (inspiration) is greater than during expiration at the same lung volumes. Different factors affect the hysteresis, as the elasticity of the lung is largely determined by the complex dynamic properties of the alveolar surface layers, which determine the surface tension inside the alveoli.

The volumes and some surfaces for a male with an FRC of 3.3 l, i.e. with dimensions as in Table 1.1, are listed in Table 1.3. These numbers are in agreement with the numbers of the "standard" male with an FRC of 3.3 l as proposed by the ICRP (1994). The difference between TLC and Residual Volume is called the Vital Capacity (VC), which is 4.64 l in the "standard" male.

Table 1.3. Airway volumes and surfaces at various levels of lung inflation.

	Inflation at Residual Volume	Inflation at FRC	Inflation at FRC plus Tidal Volume	Inflation at TLC
Total airway volume (l)	1.76	3.30	3.94	6.40
Total volume of alveoli (l)	1.28	2.48	2.89	4.89
Total airway surface (m^2)	70.6	109.3	123.5	172.0
Alveolar surface (m^2)	70.2	108.8	122.9	171.2
Transmural pressure gradient (kPa)	0.08	0.50	0.75	2.00

Normal respiratory frequencies are about 12-20 per minute at rest (ICRP, 1994). With 12 breaths per minute, i.e. $f_R = 0.2$ Hz, the volumetric flow rate V' is $f_R \cdot V_T$ = 128 ml/s (or 7.68 l/min or 0.46 m^3/hour). During exercise, the ventilation flow rate increases due to increased tidal volume and respiratory frequency (ICRP, 1994, Åstrand, 1983).

1.3 A model of the airway walls

The walls of the airways exist of surface tissue (epithelium). At most places, a liquid lining consisting of mucus covers this tissue. The epithelium rests on supportive tissue (upper airways down to the bronchioles) or it forms the boundary between the air in the lung and the blood capillaries (in the alveoli). Small, waving hair-shaped protrusions (cilia) from the upper layer of cells in the epithelium (ciliated tracheobronchial epthelial cells) move the mucus in the direction of the nasopharynx, where the mucus will be swallowed. This mucociliary transport is capable of clearing inhaled particles from the conducting airways in a few hours and is a major detoxication mechanism. Direct observations have shown that transport rates in the trachea or large bronchi in several species range from 1 to 3.5 cm/min (Menzel & Amdur, 1986). The mucous layer is divided into the hypophase, i.e. the mucus closest to the epithelium in which the cilia protrude, and the epiphase lying on top of the hypophase (Miller et.al, 1993).

This gives raise to development of a simple model of the walls of the airways, see Figure 1.4. As the physical-chemical properties of the epiphase and hypophase are probably very similar, no distinction between the two layers needs to be made. In the alveoli, the thickness h_{tissue} of the blood layer is only half the thickness of the capillary, as the other side faces the neighbouring alveolus.

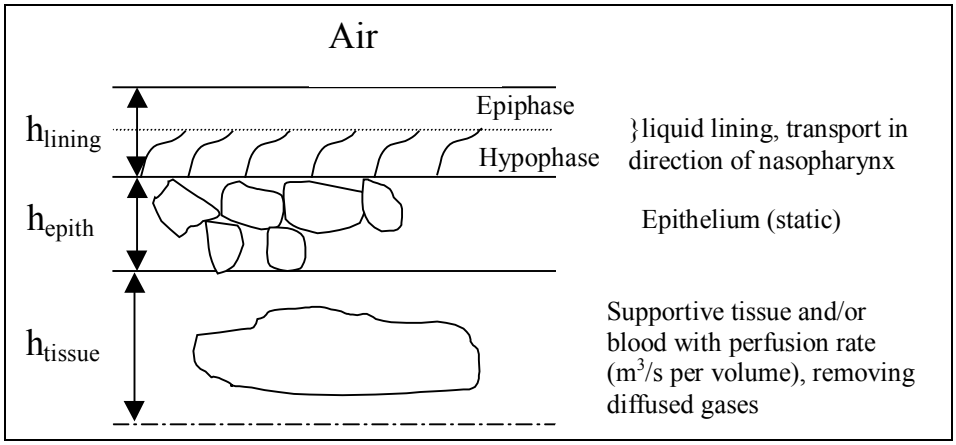

Figure 1.4. Model of the airway walls.

The liquid lining moves slowly in the direction of the nasopharynx. This means that there is a convective transport of substances in the liquid lining in that direction. All over the airway system, the thickness of the lining is maintained by secretion of mucus from the epithelium, to compensate for loss of lining due to evaporation, etc. This will not be considered, which means that we are not interested in describing the mass balance for the lining, only for the substances transported.

Around the alveoli, the substances that are diffused/absorbed in the blood (blood cells and plasma), will be removed by the blood flow (perfusion). The rate of removal of the substances is proportional to the flow rate related to the volume (or mass) of blood. Also in the other parts of the airways, the supportive tissue will be perfused at a certain rate by the blood, removing substances from the site.

To apply this model, we need information of the thickness of the layers for all elements in the airway, as well as rates for lining transport and perfusion.

The thickness of the alveolar epithelium of 0.75μm (harmonic mean) is taken from Miller et al., 1993. According to their data, the capillary lumen in a man with a FRC of 3.3 l will be about 165 ml. Assuming that the blood capillaries

can be considered as a sheet covering the alveolar surface, the thickness of this sheet can be calculated to be about 1.7 μm. This corresponds well with micrograph pictures in Weibel and Gill, 1977. With a cardiac output of 331 l/hour (Gargas et al, 1993), the perfusion rate in the lung is 0.55 s^{-1}. The velocity of the alveolar lining can be estimated using the analysis by Podgórsky and Gradón, 1993. With an average cleansing time of 60 min., the lining velocity will be about 4.8×10^{-7} m/s. According to these authors, the lining thickness is about 0.05 μm.

The remaining wall-layer thicknesses are derived from various sources, mainly micrographs. Miller et al. (1993) list lining thickness for bronchioles, bronchi and main bronchi, 1.8, 6.9, and 8.3 μm, respectively. For higher airways 10 μm is assumed, for lower airways the lining layer thickness development is distributed regularly between alveoli, bronchioles and bronchi.

Table 1.4. Dimensions and characteristics of the human airway walls at FRC. For the completely alveolated alveolar ducts, the wall properties are not relevant (grey area).

	Generation	Mucociliary velocity (mm/s)	Thickness of lining (mm)	Thickness of epithelium (mm)	Thickness supportive tissue (mm)	Mass fraction of blood in tissue	Perfusion rate per second
Mouth	-6			0.05	0.50	5%	0.0069
Nares-nasal valve	-8	-0.09	0.01	0.05	0.50	5%	0.0069
Nasal cavity	-7	-0.09	0.01	0.05	0.50	5%	0.0069
Nasopharynx	-6	-0.14	0.01	0.05	0.50	5%	0.0069
Oral pharynx	-5	-0.27	0.01	0.05	0.50	5%	0.0069
Laryngal pharynx	-4	-0.29	0.01	0.05	0.50	5%	0.0069
Vestibulum laryngis	-3	0.40	0.01	0.017	0.50	5%	0.0069
Rima glottidis	-2	1.00	0.01	0.017	0.50	5%	0.0069
Cavum laryngis	-1	0.67	0.01	0.017	0.50	5%	0.0069
Trachea	0	0.52	0.01	0.017	0.50	5%	0.0069
Main bronchi	1	0.47	0.008	0.014	0.47	5%	0.0069
Bronchi	2	0.45	0.007	0.012	0.334	5%	0.0069
Bronchi	3	0.40	0.006	0.010	0.239	5%	0.0069
Bronchi	4	0.36	0.005	8.9E-03	0.171	5%	0.0069
Bronchi	5	0.29	0.004	7.6E-03	0.139	5%	0.0069
Bronchi	6	0.23	0.004	6.6E-03	0.111	5%	0.0069
Bronchi	7	0.18	0.003	5.7E-03	0.092	5%	0.0069
Bronchi	8	0.14	0.003	5.0E-03	0.076	5%	0.0069
Bronchioles	9	0.11	0.002	4.3E-03	0.062	5%	0.0069
Bronchioles	10	0.08	0.002	3.8E-03	0.051	5%	0.0069
Bronchioles	11	0.05	0.002	3.7E-03	0.041	5%	0.0069
Bronchioles	12	0.03	0.002	3.7E-03	0.033	5%	0.0069
Bronchioles	13	0.02	0.002	3.7E-03	0.026	5%	0.0069
Bronchioles	14	0.012	0.002	3.7E-03	0.022	5%	0.0069
Terminal bronchioles	15	0.007	0.002	3.7E-03	0.020	5%	0.0069
Respiratory bronch.	16	0.003	0.002	3.7E-03	0.012	5%	0.0069
Respiratory bronch.	17	0.002	0.002	3.7E-03	6.8E-03	5%	0.0069
Respiratory bronch.	18	0.001	0.002	3.7E-03	4.0E-03	5%	0.0069
Alveolar duct	19	0.001	0.001	2.4E-03	3.2E-03	5%	0.0069
Alveolar duct	20	0.001	5.E-04	1.6E-03	2.7E-03	5%	0.0069
Alveolar duct	21	0.001	3.E-04	1.2E-03	2.5E-03	5%	0.0069
Alveolar duct	22	3.0E-04	2.E-04	1.1E-03	2.4E-03	5%	0.0069
Alveolar duct	23	1.5E-04	2.E-04	1.1E-03	2.4E-03	5%	0.0069
Alveolar sac	24	4.6E-05	2.E-04	1.1E-03	2.4E-03	5%	0.0069
Alveoli	From 16-24	4.8E-05	5.E-05	7.5E-04	1.5E-03	100%	0.55

Epithelium thickness at the nose and the trachea was derived from micrographs from St.George et al. (1993). Remaining values are interpolated between the alveoli and the trachea.

The thickness of supporting tissue is hard to determine, because at the higher level airways, the supporting tissue is attached to other tissue without a clear distinction. At the level of alveolar ducts, the tissue thickness can be thought equal to the thickness of the fibre strands around the duct entry – this is about 4 μm (micrograph from Weibel and Gill, 1977). But micrographs show that along the respiratory bronchioles, tissue thickness rapidly increases to 20 μm in the terminal bronchiole (value for cats, St.George et al., 1993). From other micrographs in the same reference, a tissue thickness of about 0.5 mm from the trachea upward seems a reasonable assumption.

To obtain a rough agreement between the mucus transport throughout the airway system (what is coming out of one element will roughly be transported further by the next element) it is necessary to assume that at each generation of bronchi and bronchioles about 10% of the mucus disappears. In this way a balance can be obtained between the cleansing time of the alveoli, the velocity of the mucociliary transport (about 3 cm/min) at the trachea, and the thickness of the lining layer (50 nm in the alveoli and about 10 μm in the trachea).

Gargas et al. (1993) list values for cardiac output and perfusion of organs. We assume that the supporting tissue of the airways can be classified as "slowly perfused organs". For a cardiac output of 331 litre/hour, perfusion of these organs will be 340 mg/(kg·s), which is represented in the model by a mass fraction of blood in tissue of 5% and a perfusion (refreshment) of this blood at a rate of 0.0069 per second.

Results for wall layer thickness and properties are indicated in Table 1.4.

1.4 Disadvantages of the selected representation of the airway system

In the selected representation of the airway system, i.e. by applying a regular branching model and having each generation of elements only represented once, some aspects of the real airway system can not be accounted for.

It appears, that normally not all parts of the lung (i.e. parts with the same generation) are ventilated at the same rate. Likewise, not all parts of the lung are equally perfused (they have a different blood flow rate), thus showing different air/blood gas exchange rates. The level of exercise is an important factor for the amount of so-called physiological dead space (dead space includes the volume of air inspired but not taking part in oxygen/carbon dioxide exchange) (ICRP, 1994).

2 Morphology of the airway system of laboratory animals

The most important laboratory animal for inhalation toxicology is the rat. An airway model of the rat that corresponds to the human model in chapter 1 from the trachea downwards was found in Yeh, Schum and Duggan (1979). Quantitative data of the dimensions of the nasal-pharyngeal passage is collected from Schreider and Raabe (1981). The data from these sources was transferred to a

rat with a weight of 300 g (Wistar rat) assuming that volume and weight are proportional. The data for Total Lung Capacity are included in Table 2.1.

For the wall thickness dimensions, the sparse information was completed assuming regular changes of dimensions along the airway elements and similarity with the airways of larger mammals (humans). With respect to airway lining, information can be found in Miller et al., 1993 for the nose (<15 μm), trachea (8-12 μm), large bronchi (5-10 μm), lobar bronchi (2-5 μm), bronchi (3 μm), bronchioles (2 μm) and terminal bronchioles (0, "no epiphase or mucus observed"). We have, despite the observation mentioned above, assumed that a regular lining layer is available down to the alveoli. For the alveoli, human values have been used.

Table 2.1. Regular branching airway morphology of a rat with a weight of 300 g and a Total Lung Capacity (TLC) of 12.9 ml (scaled to TLC)

	Generation	Total number	Number of branches	Diameter at entrance (m)	Length (m)	Fraction of surface alveolated	Number of alveoles per duct	Total number of alveoles per generation
External nares	-7	1	1	0.00196	0.00584			
Maxilloturbinate region	-6	1	1	0.00395	0.01116			
Ethmoturbinate region	-5	1	1	0.00437	0.00850			
Nasopharynx	-4	1	1	0.00213	0.01594			
Oropharynx	-3	1	1	0.00353	0.00319			
Laryngopharynx	-2	1	1	0.00337	0.00266			
Esophagus	-1	1	1	0.00165	0.00691			
Trachea	0	1	2	0.00329	0.02596			
Main bronchi	1	2	1.5	0.00281	0.00693			
Bronchi	2	3	1.67	0.00255	0.00387			
Bronchi	3	5	1.6	0.00197	0.00170			
Bronchi	4	8	1.75	0.00158	0.00201			
Bronchi	5	14	1.64	0.00130	0.00113			
Bronchi	6	23	1.65	0.00119	0.00110			
Bronchi	7	38	1.71	0.00108	0.00126			
Bronchi	8	65	1.68	9.20E-04	9.59E-04			
Bronchioles	9	109	1.69	8.43E-04	8.82E-04			
Bronchioles	10	184	1.68	7.56E-04	9.30E-04			
Bronchioles	11	309	1.69	6.78E-04	7.07E-04			
Bronchioles	12	521	1.68	5.62E-04	7.27E-04			
Bronchioles	13	877	1.68	4.75E-04	5.81E-04			
Bronchioles	14	1477	1.68	3.49E-04	5.33E-04			
Terminal bronchioles	15	2487	2	1.94E-04	3.39E-04	0	0	0
Respiratory bronch.	16	4974	2	1.65E-04	2.81E-04	0.12	6	29844
Respiratory bronch.	17	9948	2	1.55E-04	2.42E-04	0.25	9	9.0E+04
Respiratory bronch.	18	19896	2	1.45E-04	2.13E-04	0.5	14	2.8E+05
Alveolar duct	19	39792	2	1.36E-04	1.94E-04	1	24	9.6E+05
Alveolar duct	20	79584	2	1.36E-04	1.84E-04	1	24	1.9E+06
Alveolar duct	21	159168	2	1.36E-04	1.74E-04	1	24	3.8E+06
Alveolar duct	22	318337	2	1.36E-04	1.65E-04	1	24	7.6E+06
Alveolar sac	23	636673	0	1.36E-04	1.65E-04	1	24	1.5E+07
Alveoli	From 16-23			7.10E-05	6.97E-05			3.0E+07

Based on Miller et al., 1993 and Gehr et al., 1993, the epithelium thickness at the alveoli is 0.38 μm. Epithelium thickness in the nose was set at 17 μm.

The thickness of the capillary layer around the alveoli was calculated from the alveolar surface and the capillary volume and is 1.3 μm, slightly less than the

value in humans. With a cardiac output of 7.1 litre per hour, the perfusion of the alveolar sheet is 2.52 per second.

Tissue thickness at the respiratory bronchioles and the terminal bronchiole was at 17/20 part of the human values (the human value taken to be equal to values for cats, see the previous chapter). The tissue thickness above the trachea is set at 80 μm, a factor 6.25 lower than for humans (The linear scale between humans and rats, taken as the cube root of the weight ratio, is about a factor 7).

Mucociliary velocity was calculated using the same principles as for humans, based on a cleaning time of 60 min. for the alveoli.

Results are shown in Table 2.2.

Table 2.2. Dimensions and characteristics of the airway walls of rats at TLC. For the completely alveolated alveolar ducts, the wall properties are not relevant (grey area).

	Generation	Thickness of lining (mm)	Thickness of epithelium (mm)	Thickness supportive tissue (mm)	Mucociliary velocity (mm/s)	Mass fraction of blood in tissue	Perfusion rate per second
External nares	-7	0.01	0.017	0.08		5%	0.026
Maxilloturbinate region	-6	0.01	0.017	0.08		5%	0.026
Ethmoturbinate region	-5	0.01	0.017	0.08		5%	0.026
Nasopharynx	-4	0.01	0.017	0.08		5%	0.026
Oropharynx	-3	0.01	0.017	0.08		5%	0.026
Laryngopharynx	-2	0.01	0.017	0.08		5%	0.026
Esophagus	-1	0.01	0.017	0.08	1.034	5%	0.026
Trachea	0	0.01	0.017	0.08	0.470	5%	0.026
Main bronchi	1	7.5E-03	0.013	0.070	0.334	5%	0.026
Bronchi	2	5.0E-03	0.008505	0.062	0.335	5%	0.026
Bronchi	3	4.4E-03	0.007507	0.055	0.270	5%	0.026
Bronchi	4	3.8E-03	0.006632	0.048	0.218	5%	0.026
Bronchi	5	3.4E-03	0.005864	0.043	0.157	5%	0.026
Bronchi	6	3.0E-03	0.005191	0.037	0.108	5%	0.026
Bronchi	7	2.6E-03	0.0046	0.033	0.074	5%	0.026
Bronchi	8	2.3E-03	0.004082	0.029	0.053	5%	0.026
Bronchioles	9	2.0E-03	0.00363	0.026	0.036	5%	0.026
Bronchioles	10	2.0E-03	0.00363	0.023	0.021	5%	0.026
Bronchioles	11	2.0E-03	0.00363	0.020	0.013	5%	0.026
Bronchioles	12	2.0E-03	0.00363	0.018	8.4E-03	5%	0.026
Bronchioles	13	2.0E-03	0.00363	0.015	5.4E-03	5%	0.026
Bronchioles	14	2.0E-03	0.00363	0.014	4.0E-03	5%	0.026
Terminal bronchioles	15	1.4E-03	0.00271	0.012	5.4E-03	5%	0.026
Respiratory bronch.	16	1.0E-03	0.00205	6.8E-03	4.0E-03	5%	0.026
Respiratory bronch.	17	7.4E-04	1.6E-03	3.9E-03	2.7E-03	5%	0.026
Respiratory bronch.	18	5.3E-04	1.2E-03	2.2E-03	1.8E-03	5%	0.026
Alveolar duct	19	3.8E-04	1.0E-03	2.4E-03	1.2E-03	5%	0.026
Alveolar duct	20	2.7E-04	8.2E-04	2.3E-03	7.6E-04	5%	0.026
Alveolar duct	21	1.9E-04	7.0E-04	2.2E-03	4.6E-04	5%	0.026
Alveolar duct	22	1.4E-04	6.1E-04	2.2E-03	2.6E-04	5%	0.026
Alveolar sac	23	1.0E-04	5.4E-04	2.1E-03	1.1E-04	5%	0.026
Alveoli	From 16-23	5.0E-05	3.8E-04	1.3E-03	1.5E-05	100%	2.520

2.1 Respiration of the rat

We apply data for Wistar rats as observed under experimental conditions, i.e. in restraining tubes. This leads to increased respiration frequencies and inhalation, (frequency about 180-210 per min. and a tidal volume of 2 to 2.5 ml), compared to published information (160 per min. and 1.4 ml, respectively) due to some stress. The volumes and some surfaces for a Wistar rat of 300 g are summarised in Table 2.3. The transmural pressure gradients are estimated to match the required volumes. For the calculations presented in this report, an inspiration frequency of 180 per min. and a tidal volume of 2 ml are used, leading to a minute ventilation of 360 ml/min.

Table 2.3. Airway volumes and surfaces at various levels of lung inflation for a Wistar rat.

	Inflation at FRC	Inflation at FRC plus Tidal Volume	Inflation at TLC
Total airway volume (ml)	6.9	8.9	12.9
Total volume of alveoli (ml)	4.1	7.6	8.3
Total airway surface (m^2)	0.40	0.48	0.64
Alveolar surface (m^2)	0.39	0.47	0.63
Transmural pressure gradient (kPa)	0.60	1.13	2.5

3 Modeling gas flow in airways

3.1 Incompressible gas flow without mass transfer through walls

The airway system is considered as a structure of tube-like elements. These elements are linked to each other and join interface surfaces as shown in Figure 3.1. The properties of the elements that are relevant for the airflow through the system are: the elements' volume (V_1 for element 1 in Figure 3.1) and the elements' interface area (A_1 for element 1 in Figure 3.1) with the lower generation adjacent element. The interface area at the connection with the higher generation adjacent elements is also relevant, this total area is equal to the number of branches (denoted with b, see Table 1.1) times the individual interface area (A_2 in Figure 3.1) of the adjacent higher generation elements. The interface areas are defined such that the vector of total airflow into the element is perpendicular (normal) to the area, such that the nett flow into the element is $V_1 \cdot A_1$.

The maximum transmural pressure difference is in the order of 2 kPa. Relative to atmospheric pressure (100 kPa) it means that effects of compressibility are in the order of 2%. Assuming that the nose is a perfect conditioner for the inspirated air, the air at the lower elements will be at body temperature. As an acceptable simplification we will therefore assume incompressible gas flow, and in this section we will also assume that the mass transfer of gas components through the walls of the elements is zero.

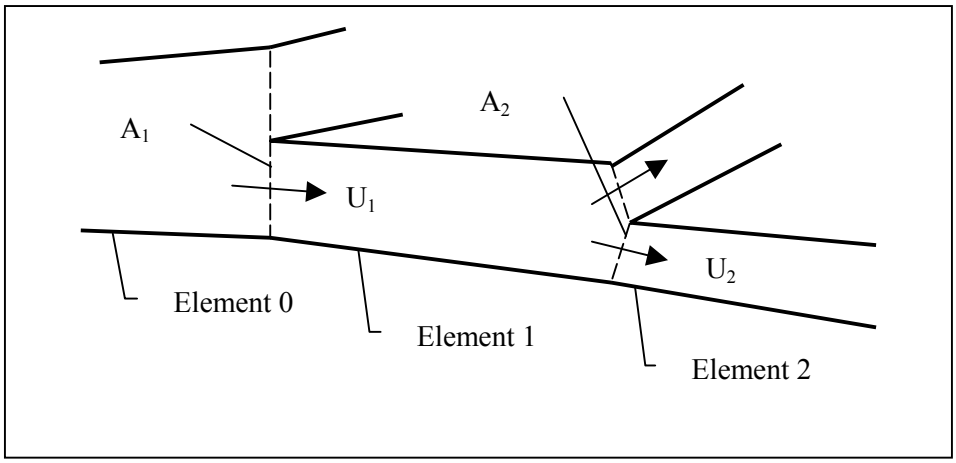

Figure 3.1. Properties of airway elements relevant for air flows.

The general balance of mass (i.e. also valid for compressible flow) for an element as shown in Figure 3.1 can be written as:

$$\frac{d\left(\langle\rho\rangle_1 V_1\right)}{dt} = \langle\rho U_1\rangle A_1 - \langle\rho U_2\rangle b_1 A_2 \qquad \textit{Equation 3.1}$$

Here, $<\rho>_1$ means averaging density over volume V_1 and $<\rho U_i>$ means averaging the product of density and velocity (normal to area A_i) over the area A_i. With ρ constant over time and volume, Equation 3.1 can be divided by ρ. This leads to the balance of volume:

$$\frac{dV}{dt} = \langle U_1\rangle A_1 - \langle U_2\rangle b_1 A_2 \qquad \textit{Equation 3.2}$$

For the highest generation, the alveoli, $U_2 = 0$. Together with this boundary condition, Equation 3.2 shows that the flow is completely dominated by the inflation of the elements. As we consider the flow to be incompressible, movements of gas are instantaneously progressing through the whole system, and neither flow resistance nor momentum plays a role. In other words, there is no need to consider the momentum balance equations in the incompressible case. Furthermore, the velocity at any interface area in the system depends only on the rate of volume change at the higher generations and can be calculated explicitly by:

$$U_i A_i = \frac{d}{dt}\left[V_i + a_i V_a + \sum_{j=i+1}^{n}\left\{\left(\prod_{k=i}^{j-1} b_k\right)\cdot\left(V_j + a_j V_a\right)\right\}\right] \qquad \textit{Equation 3.3}$$

Here, a_i is the number of alveoli at generation number i (a_i is only non-zero for the respiratory bronchioles and alveolar ducts and sacs, see Table 1.1). V_a is the volume of a single alveolus and n is the highest generation number of the airway system (n=24 according to Table 1.1 for the human airways, the highest generation number is the number of the alveolar sacs, i.e. the alveoli are not counted as they appear separately in the equation).

According to Equation 1.1, the change of volume can be related to the change of transmural pressure gradient. It should be noted that this relation neglects the hysteresis and other dynamic effects on the elasticity of the lung. This relation should therefore mainly be interpreted as a means to compare the relative changes of volumes of the elements with each other, rather than as a means to link pressure forces to the gas flow:

$$\frac{dV_k}{dt} = \left\{ {\alpha_k}^2 (1-\alpha_k) \left(\frac{P}{P_{TLC}} \right)^{-2/3} + 2\alpha_k (1-\alpha_k)^2 \left(\frac{P}{P_{TLC}} \right)^{-1/3} + (1-\alpha_k)^3 \right\} \cdot \frac{V_{TLC,k}}{P_{TLC}} \frac{dP}{dt}$$

Equation 3.4

4 Gas-phase transport and diffusion in the airways

4.1 Transport and diffusion of inert, insoluble substances in incompressible flow

The simplest case of mass transport is related to substances that don't react and that don't migrate through the walls of the elements. This means that one can write a mass balance that only takes into account convection of material with the main gas flow and gas-phase diffusion.

In addition to the properties relevant to gas flow, it is necessary to define the length (l) of the element. Furthermore, the mass concentration (C) is primarily defined at the centre of the element. Two remarks need to be made here. First, as for density, we need to average concentration over volume, denoted by $<C>_i$ for element i. Furthermore; we also need the concentration defined at the interface area, because this quantity is convected by the main flow. C_{01} and C_{12} will denote these concentrations at the upper (with lower generation numbers) and lower (with higher generation numbers) interfaces, respectively. In this case the definition will involve some averaging over the interface areas. The properties are indicated in Figure 4.1.

Assuming incompressible flow, the component mass balance for element 1 as in Figure 4.1 can be written as follows. The definitions of <..> and $<..>_1$ (area and volume averaging, respectively) are as in chapter 3:

$$\frac{d(<\rho C>_1 V)}{dt} = <C_{01}U_1>\rho A_1 - <C_{12}U_2>\rho b_1 A_2 + \rho D\left[\frac{\Delta <C_{01}>}{s_{01}} A_1 - \frac{\Delta <C_{12}>}{s_{12}} b A_2 \right]$$

Equation 4.1

Here, D is the diffusion coefficient for the component in the gas phase (typically air). The terms Δ<C> represent the concentration gradient across the interfaces and s_{01} and s_{12} are the corresponding distances between the elements over which

the diffusion takes place. In order to express all concentrations using the values in the elements' centres, we need to make the assumption that <CU> over an interface area can be replaced by <C><U>. This is not necessarily true, as variations of U and C in radial direction might be correlated, but for most relevant flow regimes it is a reasonable assumption.

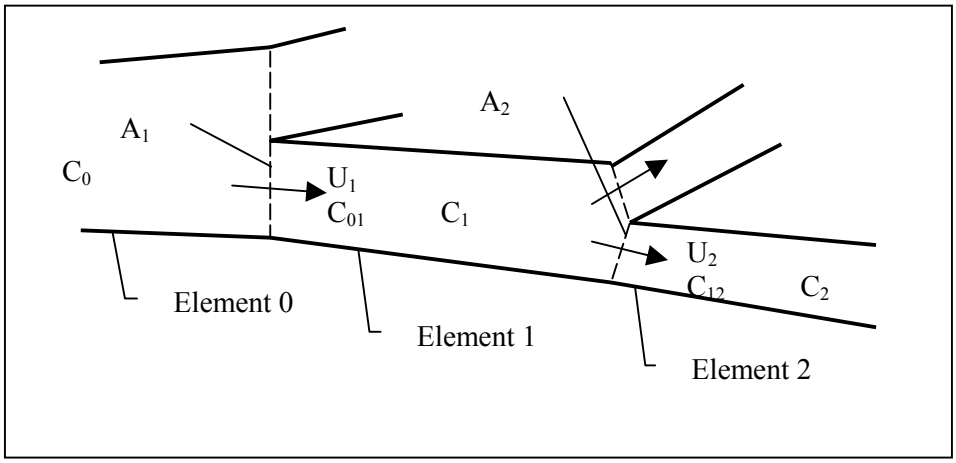

Figure 4.1. Properties of elements relevant to mass transport and diffusion.

For a stable numerical solution, it appears that we need upwind differencing for the advective terms: $\langle C_{01} \rangle = ((1+\delta)\cdot\langle C \rangle_0 + (1-\delta)\langle C \rangle_1)/2$ with $\delta=1$ if velocity is from element 0 to 1 and $\delta=-1$ if velocity is from 1 to 0.

The gradient diffusion terms can be substituted using the differences of the centre concentrations, and the distances s_{01} and s_{12} both by half the sum of the elements' lengths. For easier reading, we substitute $\langle C \rangle_i$ by C_i and $\langle U_i \rangle$ by U_i. With this, the convection-diffusion equation can be written as:

$$\rho V_1 \frac{dC_1}{dt} = -\rho C_1 \frac{dV_1}{dt} + \rho U_1 A_1 \frac{(1+\delta)C_0 + (1-\delta)C_1}{2} - \rho U_2 b A_2 \frac{(1+\delta)C_1 + (1-\delta)C_2}{2} + 2\rho D\left(\frac{C_0 - C_1}{l_0 + l_1} A_1 - \frac{C_1 - C_2}{l_1 + l_2} b A_2\right) \qquad \textit{Equation 4.2}$$

The above equation leads to a set of coupled, 1st order ordinary differential equations that need to be solved by numerical integration over time. Volumes, areas, lengths and velocities can be calculated directly (see section 3.1). The boundary condition for the set of equations is the external concentration (the concentration at the mouth or nose).

Using an explicit Runge-Kutta integration scheme, a stable numerical time step is approximated by:

$$\Delta t < 1.4\frac{l^2}{D} \text{ and } \Delta t < \frac{2.8}{\left|-2\frac{D}{l^2} - \sqrt{\frac{4D^2}{l^4} - \frac{U^2}{l^2}}\right|}$$

Taking values at the alveolar level ($l \approx d \approx 300\mu m$), the time step should be less than about 0.01 s.

4.2 Transverse diffusion of gases to tissue surrounding the airways

Based on the model for the airway walls, we can describe diffusion of substance to and through the walls. We define bulk concentration values in the centres of the layers identified in Figure 1.4, see Figure 4.2.

Transverse diffusion in the airway itself is a combination of turbulent diffusion and molecular diffusion. We assume that the turbulent region is well mixed (infinitely large diffusion coefficient). In case there is a turbulent region in the core of the airway tube, the diffusion path length is assumed to be equal to the thickness of the viscous layer. The thickness of the viscous layer can be estimated from (Tennekes & Lumley, 1974):

$$h_{visc} = 5\frac{\nu}{u_*}$$

$$u_* = \frac{U_{bulk}}{2.5 \cdot \ln(\frac{d \cdot u_*}{2 \cdot \nu}) + 1.5} \qquad \textit{Equation 4.3}$$

Here, ν is the kinematic viscosity of the air (about $15 \cdot 10^{-6}$ m^2/s), u_* is the scale of the turbulent fluctuations, U_{bulk} is the bulk velocity of the air within the airway (as calculated by Equation 3.3).

If there isn't a turbulent core in the flow, then the concentration profile will take a parabolic shape, where the maximum concentration is 2 times the bulk concentration (when the concentration at the wall is zero). The bulk concentration can be found at a distance of $\sqrt{½}$ times the radius from the centre, in other words, the effective value of h_{visc} is 0.147 times the diameter.

For complexly shaped elements, like the nose, an effective "hydraulic" diameter is used to determine h_{visc} using Equation 4.3. This diameter is derived from the assumption that the complex shape can be represented by a tube with an ellipsoid cross section, in such a way, that surface and volume of the element matches the values listed in Table 1.2. The area of and ellipse equals $\pi \cdot a \cdot b$, the circumference of an ellipse is approximated as $2 \cdot \pi \cdot \sqrt{(a^2 + b^2)}$, where a and b are the short and long axis of the ellipse. The short axis is used in determination of h_{visc}, as it gives an indication of the average width of the flow channel.

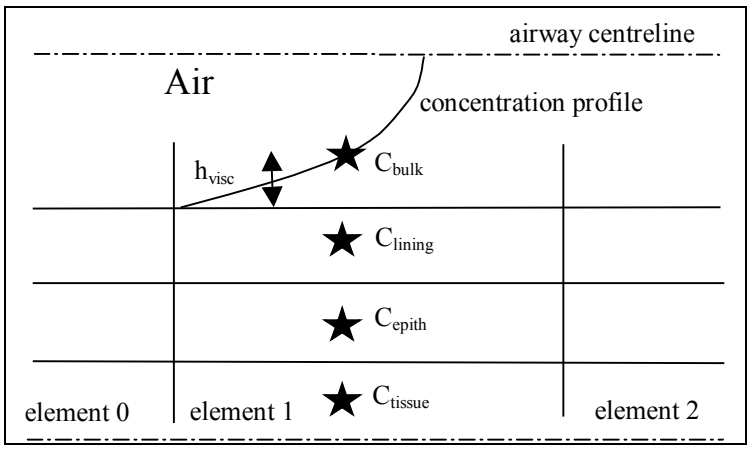

Figure 4.2. Definition of bulk concentrations in the airways

The diffusive flow between the wall layers is determined by the differences between the bulk concentrations in these wall layers, corrected by the equilibrium partition coefficients (or Henry constants) between the layers. At the interface between the layers there will be local equilibrium. Using this, one can write for the mass flux of a substance m' (in kg $s^{-1}m^{-2}$) between the air inside the airway and the lining:

$$m'_{air \to lining} = \frac{C_{bulk} - \lambda_{air/lining} C_{lining}}{\frac{h_{visc}}{\rho_{air} D_{air}} + \frac{\lambda_{air/lining} h_{lining}}{2\rho_{lining} D_{lining}}} \qquad \textit{Equation 4.4}$$

Here, $\lambda_{air/lining}$ is the partition coefficient between air and the lining for the substance in question. ρ_{air} and ρ_{lining} are the densities of air and lining and D_{air} and D_{lining} are the diffusion coefficients for the substance in air and in the lining, respectively. The thicknesses h are according to Figure 1.4 and Figure 4.2. For the other interfaces, similar expressions can be derived.

In principle, using bulk properties for the layer compartments will overestimate the diffusion through the layers (numerical diffusion due to course discretisation). Morris, Hassett and Blanchard (1993) refer to studies that show that these effects are small if the compartment thickness is less than 10 μm. In this application, compartment thickness may well be more than 10 μm, but at this state of modelling, we refrain from dividing layers into smaller elements.

The general formulation for the mass balance in a wall layer of an element of the airway can be written as follows:

$$\begin{aligned} \frac{dm_{i,1}}{dt} = h_{i,1} A_{peri,1} \rho_i \frac{dC_{i,1}}{dt} = (m'_{i-1 \to i} - m'_{i \to i+1}) A_{peri,1} + \\ \rho_i U_{i,1} \frac{h_{i,1} A_{peri,1}}{l_1} \frac{(1-\delta_i) C_{i,0} + (1+\delta_i) C_{i,1}}{2} - \\ \rho_i U_{i,2} b \frac{h_{i,2} A_{peri,2}}{l_2} \frac{(1-\delta_i) C_{i,1} + (1+\delta_i) C_{i,2}}{2} - \\ \frac{f_i q_i h_{i,1} A_{peri,1} \rho_i (C_{i,1} - \lambda_{i/blood} C_{venous})}{\lambda_{i/blood}} \end{aligned} \qquad \textit{Equation 4.5}$$

Here, A_{peri} is the peripheral surface of the airway element, ρ_i is the density and U_i is the velocity of layer i (U_i is only relevant for the lining) with δ_i the upwind-differencing factor: if $U_i > 0$, $\delta_i = 1$, otherwise $\delta_i = -1$. The last term is only relevant for the perfused tissue: it presents the removal of substance by blood. The symbol f_i denotes the mass fraction of blood in the tissue and q_i is the local perfusion rate (s^{-1}). C_{venous} is the concentration in the blood. For the alveolar region, this will be the venous concentration. For parts higher up in the airway system, this may be the arterial concentration, but for convenience a single value is used for the whole system. (Note that C_{venous} will be time dependent as the last term of Equation 4.4 actual contributes to mass transfer from the airway wall into the body.)

Now an additional term is needed in Equation 4.2 to account for the removal of material from the air to the wall. This term is actually the mass flow represented by Equation 4.4: $-m'_{air \to lining} A_{peri}$.

The time scales related to diffusion through the walls in the lower part of the airway are very small, for the alveoli in the order of 10^{-6} seconds. In order to enforce larger time steps in the numerical procedure than implied by this time scale, we prescribe equilibrium conditions in those cases when the time step is larger than the time scale. In case of total equilibrium through the entire air/blood barrier the concentration distribution through the wall layers corresponds to an equilibrium transport of substance from the air to the blood:

$$m'_{equilibrium} = m'_{air \rightarrow lining} = m'_{lining \rightarrow epith} = m'_{epith \rightarrow tissue} = m'_{tissue \rightarrow blood}$$

This equilibrium mass flux can be calculated from the concentration gradient between air and the blood, divided by the total transport resistance $R_{air/blood}$:

$$m'_{equilibrium} = \frac{C_{air} - \lambda_{air/blood} C_{venous}}{R_{air/blood}},$$

$$R_{air/blood} = \frac{h_{visc}}{\rho_{air} D_{air}} + \frac{\lambda_{air/lining} h_{lining}}{\rho_{lining} D_{lining}} + \frac{\lambda_{air/epith} h_{epith}}{\rho_{epith} D_{epith}} + \frac{\lambda_{air/tissue} h_{tissue}}{2\rho_{tissue} D_{tissue}} + \frac{\lambda_{air/blood}}{h_{tissue} \rho_{tissue} f_{tissue} q_{tissue}} \qquad \textit{Equation 4.6}$$

4.3 Other similar modelling approaches

The model presented here is very similar to an approach by Miller et al. (1985). They also divided the airway system longitudinally in elements corresponding to the generations. Air, lining (mucus or surfactant), and tissue are distinguished as different compartments in transverse direction. For this system the diffusion equation is solved, using a forced velocity distribution. Inflation is not included, but corrections to the molecular diffusion are applied instead. The model is primarily used to describe the uptake of ozone. As ozone is very reactive, the chemical reaction is of primary importance and as "dose" is actually defined as the uptake by chemical reactions in a compartment, the published results are difficult to compare to the present model. One result that probably can be taken over to our study is, that results are not sensitive to gas-phase molecular diffusion and mass transport.

Johansson (1991) also used a similar approach to model the uptake of solvents. In this case, airway elements beyond generation 5 are grouped together such that the model treats 9 "regions", the last region representing the alveoli. The gas phase and a 1-μm thick, inner layer of lining (mucus) are considered to be in equilibrium, while diffusion to a 15-μm outer wall layer is included in the upper 8 regions. In the 9th region, immediate equilibrium between alveolar air and arterial blood is assumed. Thickness of inner and outer wall layer as well as the gas phase/wall transfer coefficient were obtained by fitting the results with observations for acetone, diethyl ether and ethanol (see also chapter 5).

5 Evaluation of the airway diffusion model

There is little information available that can be used to evaluate the airway diffusion model. Measurements of internal doses (i.e. concentrations inside the airways and the airway wall tissue) could not be traced in the literature.

Only observations of concentration in exhaled air following exposure of some substances are available. These observation indirectly show absorption in the air way system, albeit that little information can be derived with respect to the site of absorption. Schrikker et al. (1985) report measurements of the uptake of acetone and diethylether by male humans over short periods (exposure duration 40 s). This includes presentation of the concentration traces in the inhaled and exhaled air, which allows analysing what happens during a single breath. The next 2 sections will show how our model compares with these measurements.

Johanson (1991, see section 4.3) has also used these measurements to develop and evaluate a model that shows resemblance with our model, albeit that only 9 compartments are distinguished compared to the more than 30 elements in our representation of the airways, and the airway walls contain one compartment only. Johanson used Schrikker et al.'s (1985) data to fit the rate of diffusion from the air to the wall.

Other experimental data is available from Nodelman & Ultman (1999). Small amounts of chlorine were injected as "boluses" at different moments during the inhalation cycle and the exhaled air analysed for the non-absorbed chlorine. By varying the time of injection, some control was obtained about the penetration of the chlorine in the (upper) airways and thus about the different absorption rates along several airway elements. This study concentrated on absorption in the nasal and oral area. Some results will be discussed in section 5.3.

5.1 Diethylether

Table 5.1. Physical properties for diethylether and acetone as used for evaluation of the model.

	diethylether	acetone
Partition coefficient λ_{al} (kg/kg in air)/(kg/kg in water), 37 ºC	67.01 (Fiserova-Bergova, 1983)	2.225 (Fiserova-Bergova, 1983)
Partition coefficient λ_{et} (kg/kg in water)/(kg/kg in tissue), 37 ºC	1.081 (Fiserova-Bergova, 1983)	1.661 (Fiserova-Bergova, 1983)
Diffusion coefficient in air (m^2/s)	$9.5 \cdot 10^{-6}$ (Johanson, 1991)	$7.9 \cdot 10^{-6}$ (Johanson, 1991)
Diffusion coefficient in lining, epithelium and tissue (m^2/s)	$0.832 \cdot 10^{-9}$ (find reference)	$1.085 \cdot 10^{-9}$ (find reference)

The physical properties of acetone and diethylether are listed in Table 5.1. It should be noted that a low value of the partition coefficient λ_{al} corresponds to a high concentration in the lining that is in equilibrium with the gas phase. In order words, low values of λ_{al} indicate that the substance easily dissolves in the

lining (water)[1]. Acetone dissolves easier in water than ether. This has considerable consequences for the internal dose of the airway walls and the uptake of the substance, as we will show.

First, the comparison of calculations and measurements for diethylether is shown. The measurements and simulation are based on a mouth-breathing human male, exercising at 50W, pulmonary ventilation 25.2 l/min, cardiac output 9.9 l/min and a breathing frequency of 18.2 per minute.

The results are shown in Figure 5.1. This Figure shows some experimental problems. The concentration in inhaled air (taken directly from Schrikker et al., 1985) should be at 100% of the exposed concentration. Johanson (1991) adjusted the concentration scale as to reproduce the inhaled concentration as $C/C_{exposure}=1$. This would increase all measured concentrations by 10%. Considering this, the calculations fit very well to the measurements. The averaged concentration in exhaled air after the first 4 breaths, when steady state seems to be reached, is calculated to be $0.33 \cdot C_{exposure}$, equal to the measured value if we correct with the above 10%. Also the minimum exhaled concentration agrees very well.

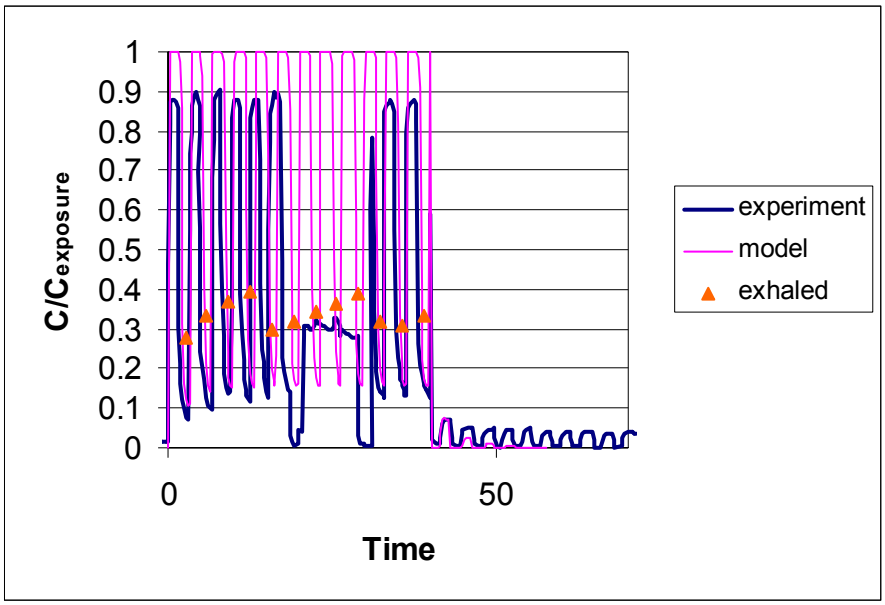

Figure 5.1. Comparison of measured (Schrikker et al., 1985) and calculated concentrations of diethylether in inhaled and exhaled air. Exposure duration is 40 s. After the 6th breath, the averaged exhaled concentration was measured directly over 4 breaths.

An analysis of the calculation results for concentrations inside the airways shows that the end-exhaled concentration equals the alveolar concentration. This means that there is almost no interference of absorption in the elements of the upper airway on the uptake and washout of diethylether. The alveolar concentration can be estimated from the total mass flow (uptake) of ether and the partition coefficient from air to blood. From the equilibrium between concentration in alveolar air and blood it follows that $C_{alveolar\ air} = \lambda_{air/blood} \cdot C_{alveolar\ blood}$. From the mass balance $Q_{air} \cdot (C_{exposure} - C_{alveolar\ air}) = Q_{blood} \cdot (C_{alveolar\ blood} - C_{venous})$,

1 In this report all concentrations and therefore also partition coefficients are based on mass concentrations. As partition coefficients often are based on volume concentrations and/or partial pressures, values for partition coefficients in this report seem roughly a factor 1000 larger than normally encountered in literature due to the ratio of densities for air and water.

with Q_{air} and Q_{blood} the pulmonary ventilation and cardiac output in kg/s, respectively, it follows that, assuming $C_{venous} = 0$:

$$\frac{C_{alveolar\ air}}{C_{exposure}} = \frac{\frac{Q_{air}}{Q_{blood}}\lambda_{air/blood}}{1+\frac{Q_{air}}{Q_{blood}}\lambda_{air/blood}} \qquad \textit{Equation 5.1}$$

For this case, the alveolar concentration can be estimated to be $0.15 \cdot C_{exposure}$ on average. *Figure 5.2* shows that according to the model calculations, during exhalation the concentration in the lowest part of the lung falls to about 10% of the exposure concentration $C_{exposure}$. During exhalation there is only a small concentration gradient in the airway: from around 10% at the alveoli to about 15% at the mouth. During inhalation the concentration in the upper airways again show almost no gradient until the first respiratory bronchiole (the first airway element with some alveoli), indicating that there is almost no uptake at the upper level elements. From here, the concentration during inhalation reduces rapidly from almost 100% at the first respiratory bronchiole to 15% at the alveolar sacs. This result is in agreement with the results obtained by Johanson (1991). In Johanson's case, the alveolar region is represented by only one element. In this region, variations during inhalation and exhalation are predicted from 25% to 15%, respectively.

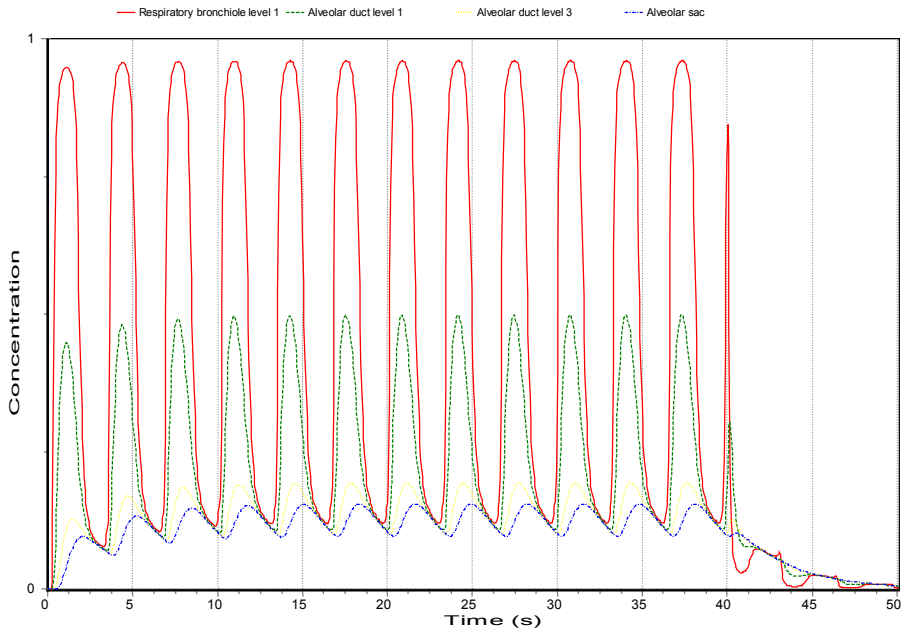

Figure 5.2. Gas phase concentration of diethylether in the lower part of the respiratory system

5.2 Acetone

The experimental conditions during the inhalation tests with acetone were identical to the conditions for diethylether. The results of the experiments and the model calculations are shown in Figure 5.3. It appears that in this case the agreement between the model results and the experiments is less good. In the case of a well soluble vapour like acetone, the concentration of mixed-exhaled and end-exhaled air is not determined by the alveolar concentration, but by the absorption (during inhalation) and desorption (during exhalation) of the upper

airway walls. A correct description of the concentration in the exhaled air depends on the correctness of the description of the lateral diffusion processes in the upper airways. Johanson (1991) reached good agreement, but it should be noted that he used the measurements to adjust the diffusion rate from the gas phase to the walls, so his results can not be considered as a blind evaluation.

According to Equation 5.1, the concentration in the alveolar region would be about 1% of the exposure concentration. In practice, the concentration does not penetrate beyond the first alveolar ducts, with almost zero concentrations at lower levels. The concentration is already significantly reduced in the upper airways. At the terminal bronchiole, concentration varies between 20% and 60% during inhalation and exhalation, respectively. For the corresponding region, Johanson (1991) predicts a variation between 20% and 70%.

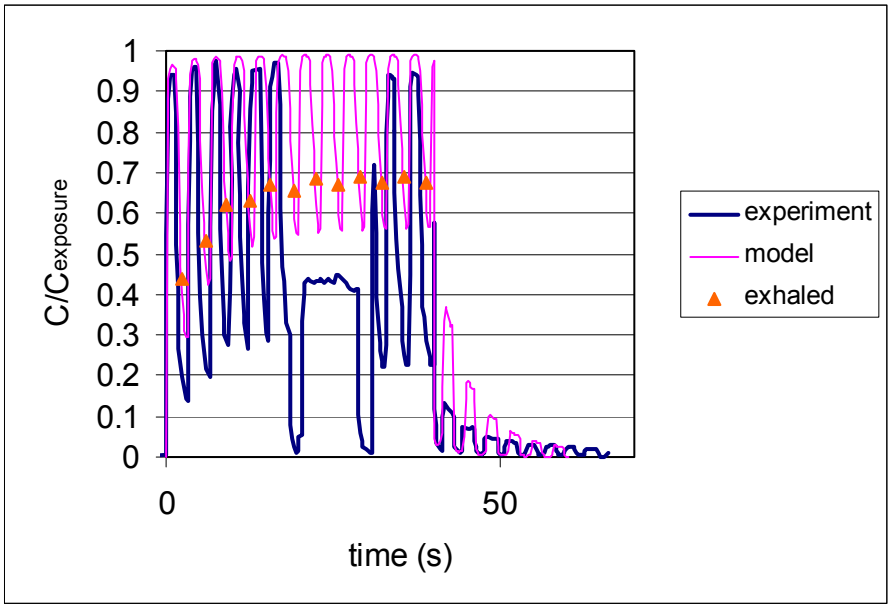

Figure 5.3. Comparison of measured (Schrikker et al., 1985) and calculated concentrations of acetone in inhaled and exhaled air. Exposure duration is 40 s. After the 6th breath, the averaged exhaled concentration was measured directly over 4 breaths.

In view of the poor agreement between the calculations and the measurements some sensitivity calculations were performed. These calculations included the following parameter variations:

1. Maximising the thickness of the lining, epithelium and supporting tissue to 5 µm for each layer. In Johanson's (1991) model, a 1-µm layer is thought to be in instantaneous equilibrium with the gas phase, with a buffer layer of 15 µm behind it. It can be expected that the thickness of the wall layers have an effect on the amount of acetone absorbed and desorbed, and thus affect the concentration in exhaled air.
2. Decreasing the diffusion coefficient in air by a factor of 10, thus simulating reduced mass transfer from the air to the wall layer.
3. Decreasing the diffusion coefficient in lining, epithelium and tissue by a factor of 10, decreasing the mass transfer through the wall layers.

Results for the sensitivity calculations are included in Table 5.2. Although limiting the wall layer thickness has a significant effect on the end-exhaled concentration, only reducing the diffusion coefficient has a significant effect on both mixed-exhaled and end-exhaled concentrations. The question is whether a re-

duced diffusion coefficient (compared to diffusion in water) is realistic. Miller et al. (1993) state that diffusion in tissue is generally lower than in water "but often not much different". For oxygen, the lowest measured value of the diffusion coefficient in tissue (which appeared to be in dog connective tissue) is a factor 3 lower than in water. Miller et al. conclude: "For large molecules, diffusion coefficients in biological substances may be very different from the water values, making measurements in biological tissues and fluids necessary".

Table 5.2. Comparison of experiment and sensitivity calculations for acetone.

	Averaged (mixed) exhaled concentration	Minimum (end) exhaled concentration
Experiments (Schrikker et al., 1985)	0.44	0.22-0.28
Standard model calculation	0.68	0.56
Wall thickness maximised at 15 μm	0.69	0.46
Air diffusion coefficient at onetenth	0.67	0.57
Lining/tissue diffusion coefficient at onetenth	0.56	0.37

Table 5.3. Time scales for diffusion for a number of wall layer elements and 2 values of the diffusion coefficient.

	Time scales (s)			
	Diffusion coefficient $1.085 \cdot 10^{-9}$ m^2/s (acetone in water)		Diffusion coefficient $1.085 \cdot 10^{-10}$ m^2/s	
	epithelium	supporting tissue	epithelium	supporting tissue
Mouth/Nares-nasal valve to laryngal pharynx	2.30	230	23.0	2304
Trachea	0.27	230	2.66	2304
Main bronchi	0.19	208	1.87	2078
Bronchioles 1st level	0.017	3.58	0.17	35.8
Terminal bronchioles	0.012	0.37	0.12	3.69
Respiratory bronchiole 3rd level	0.012	0.015	0.12	0.15

In any case, changing the diffusion coefficients by a factor of 10 has significant effects on the time scales needed to reach equilibrium with the gas-phase concentrations. The time scale for an individual wall layer is h^2/D. For some typical elements the time scales for diffusion into the wall layers are presented in Table 5.3.

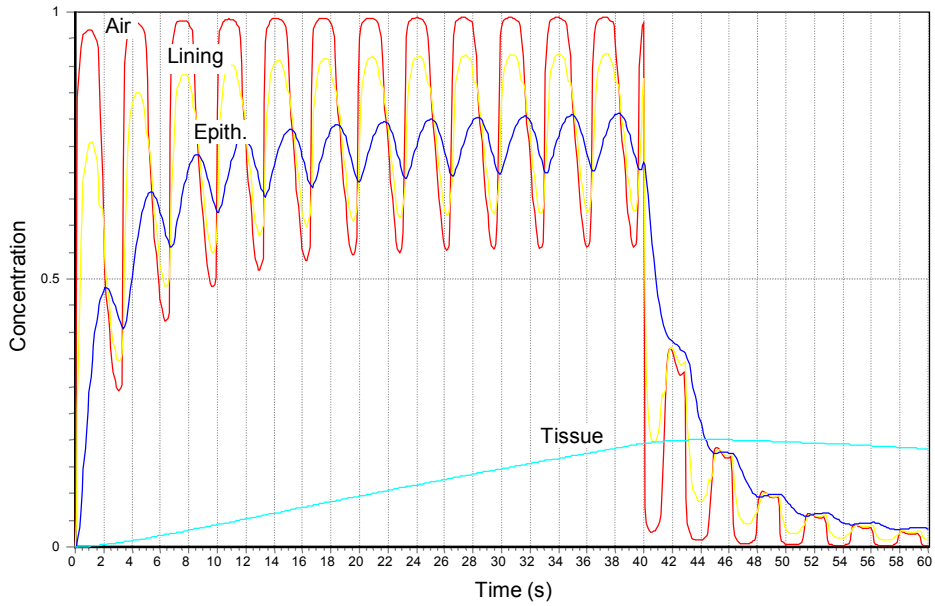

Figure 5.4. Concentration of acetone in the mouth as calculated using the standard model and the diffusion coefficient for water. Concentrations in lining, epithelium and tissue have been multiplied by the partition coefficient as to show deviation from equilibrium.

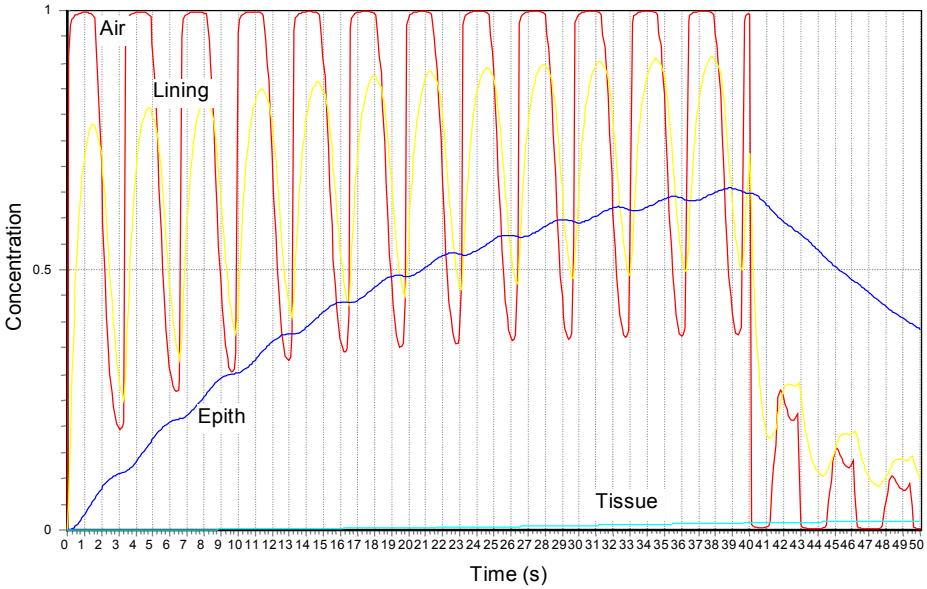

Figure 5.5. Concentration of acetone in the mouth as calculated using a diffusion coefficient for lining, epithelium and tissue that is one-tenth of the value for water. Concentrations in lining, epithelium and tissue have been multiplied by the partition coefficient.

The effect on the concentration in the wall layers is also presented in Figure 5.4 and Figure 5.5. As one can see, the conclusions on how fast the epithelium layer reaches equilibrium with the concentration in the gas phase changes drastically. Using the diffusion coefficient for water, the concentration in the mouth or nose and the airways above the trachea reaches equilibrium in the course of a single breath. If the diffusion coefficient is reduced by a factor 10, it will take about half a minute. We can conclude that the diffusion coefficient is a critical parameter in order to assess the correct internal dose in the upper airways.

5.3 Chlorine absorption in the nasal area

Measurements from Nodelman & Ultman (1999) were used to compare with model calculations of absorption of chlorine during a single inhalation/exhalation cycle. Small amounts of chlorine were injected in the inhaled air as small "boluses" of gas at different moments before the end of inhalation. The moment of injection determines the penetration of the chlorine in the airway. The inhaled volume since the gas injection is defined as the Penetration Volume. The exhaled gas is analysed for remaining chlorine and in this way absorption of chlorine depending on penetration can be determined. As the volume of the upper airway elements (nares, nasal cavity and nasopharynx) is known, see Table 1.2, information is obtained about the level of absorption along these elements. Results are shown in Figure 5.6. The comparison is difficult because of the complex physical/chemical behaviour of chlorine.

Solubility of chlorine is determined by hydrolysis, i.e. the formation of chlorine and hydrogen ions (Cl^- and H^+) and hypochloride (HOCl), see Whitney & Vivian (1941). As a result, the partition coefficient depends on the amount of chlorine (in molecular and hydrolysed form) in the solution, such that the partition coefficient approaches zero for low concentrations (i.e. infinite solubility). At the exposed concentrations of 3 ppm, the partition coefficient is about 1, for 0.5 ppm it is only 0.25 (based on mass concentrations). Nodelman & Ultman argue that on the bases of the buffering capacity (pH remains constant at 6.6) and the high natural content of chlorine ions (0.16 mol/l) the partition coefficient for the air/mucus system is constant however, independent of the exposure concentration. This is supported by the fact that the reported measurements are the same for bolus concentrations of 0.5 and 3 ppm. Based on the data from Whitney & Vivian, we estimate this constant partition coefficient to be about 6 for the mucus conditions mentioned by Nodelman & Ultman.

Another complicating factor is that hypochloride is a very reactive, oxidising substance, and we expect that it will almost instantly react with substances present in the mucus and epithelium. These will be irreversible reactions, leading to a constant sink of hypochloride in the lining and epithelium. Our model, which does not contain irreversible chemical reactions as by now, can not describe this aspect.

The model results shown in Figure 5.6 are produced using a constant partition coefficient of 1 (kg Cl_2/kg air per kg Cl_2/kg lining). The respiratory frequency is 30 per minute and the tidal volume is 500 ml, this means a ventilation flow rate of 250 ml/s. Figure 5.6 shows absorption of chlorine during one inhalation/exhalation cycle. The chlorine bolus is injected at the end of the inhalation phase of this cycle. A penetration volume of zero means that the injection takes place just as the inhalation stops and exhalation starts.

We show two types of results. The first result is the maximum absorbed amount of chlorine in the lining, epithelium and tissue during the respiration cycle. This maximum is found some 10-100 ms after the start of exhalation. After that maximum is reached, the exhaled air with low chlorine concentration

(from the deeper airways) will desorb the chlorine. This maximum absorbed fraction would be an indicator of absorption if all absorbed chlorine were bounded in the lining and other tissue.

The other result is the absorbed fraction at the end of the respiration cycle. This includes the desorbtion during exhalation.

It seems that the results for end-exhaled absorption follow the observed dependency on the penetration volume best, while the maximum absorption is in better agreement with the asymptotic results for large penetration volumes. The importance of this comparison is limited, however, because of the large uncertainty in the value of the partition coefficient, which is an important parameter for absorption.

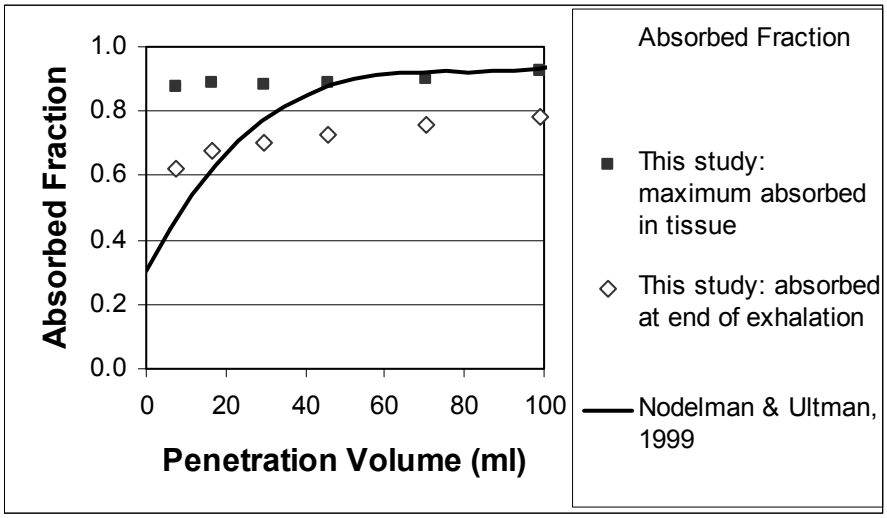

Figure 5.6. Comparison between measured and calculated chlorine absorption as function of the penetration of chlorine in the nasal area.

5.4 Discussion of the evaluation

It appears that the model reproduces uptake of gases in the lower parts (alveolar region) very well. There is however quite some uncertainty about the correctness of the model for very soluble substances and the corresponding absorption in the oral or nasal region.

Correct values for the partition coefficients for the air/lining and lining/tissue systems are very important. The sensitivity study also shows the relevance of diffusivity in lining and tissues compared to thickness of lining and tissue layers in the case of reversible absorption and desorption.

Possible improvements of the model are:

- Using detailed substance-dependent data on solubility and diffusivity in lining, epithelium and tissue.
- Using better geometrical descriptions of the elements (especially in the oral and nasal region) and their wall compartment thickness.
- Using empirical mass transport rates in the nasal/oral regions in stead of using correlations for pipe flow as described in section 4.2.
- Including chemical reactions as a “sink” of absorbed material. However, this requires detailed information of chemical reactivity in the wall layers.

6 Assessment of the selected substances

6.1 Substance properties

The following substances are selected for detailed study in the TEARHS project:

- hydrochloric acid (HCl),
- ammonia (NH_3) ,
- chlorine (Cl_2),
- phosgene ($COCl_2$),
- hydrogen-disulphide (H_2S), and
- sulphur-dioxide (SO_2).

In order to perform calculations with the airway diffusion model, the relevant properties were collected. Data source for these properties are Miller et al. (1993), Landolt-Börnstein (1962, 1969), Handbook of Chemistry & Physics (1999 p 6-190), Linke Seidel (1958), and Meylan & Howard (1991). These properties are summarised in Table 6.1. In those cases that the partition coefficient is not constant, it has been pursued to provide values for low concentration ranges. Partition coefficients are not appropriate and should be used with care in case chemical reactions are involved in the solution process (Miller et al., 1993). This is e.g. the case for chlorine, sulphur-dioxide, and phosgene. Chlorine and phosgene will be hydrolysed, forming hydrochloric acid in the aqueous phase, see section 5.3 and chapter 9.

Table 6.1. Physical properties of the selected substances.

Substance	mol weight (kg/kmol)	Partition co-efficient λ_{aw} at 37 ºC (kg/kg air per kg/kg water)	Diffusion co-efficient in water (m^2/s)	Diffusion co-efficient in air (m^2/s) at 37 ºC
HCl	36.5	1.55 *	$3.87 \cdot 10^{-9}$ at 35 ºC**	ca. $1.8 \cdot 10^{-5}$
NH_3	17	0.97	$1.5 \cdot 10^{-9}$ at 20 ºC	$2.5 \cdot 10^{-5}$ ±10%
Cl_2	70.9	strongly varying for low concentrations *	$1.8 \cdot 10^{-9}$±6% at 35 ºC	$1.27 \cdot 10^{-5}$ ±3%
$COCl_2$	98.9	184 (25ºC)	unknown	$1.73 \cdot 10^{-5}$ (temperature unknown)
H_2S	34.1	410±30	$1.36 \cdot 10^{-9}$ at 25 ºC	$1.8 \cdot 10^{-5}$ ±5%
SO_2	64.1	42*	$2.5 \cdot 10^{-9}$ at 37 ºC	$1.17 \cdot 10^{-5}$ ±15%

* Henry law is not valid (i.e. partition coefficient depends on gas-phase and liquid-phase concentration).

**For low concentrations.

The behaviour of substances in the airways is dominated by the solubility. The partition coefficient expresses the solubility. In the table above one can distinguish two or three groups. Clearly distinguishable are the very easily soluble substances (ammonia, chlorine and hydrochloric acid) with partition coefficients in the order of 1 based on mass concentrations. One can divide the re-

maining substances into easily soluble substances with a partition coefficient of 50-200 (sulphur-dioxide, phosgene), and slightly soluble substances with partition coefficients higher than ca. 500 (hydrogen-sulphide, maybe phosgene).

For comparison it should be noted that oxygen should be considered to be a "hardly soluble" gas with a partition coefficient of 37,000.

Internal exposure of the tissue in the airways is calculated for ammonia, representing very easily soluble gases, and for sulphur dioxide, representing easily soluble gases. Some additional calculations are performed for hydrogen-sulphide. Therefore we used the model described in the chapters 3 to 5. These calculations focused on assessing the time-scales for different parts of the airways, i.e. estimates of the time needed to reach the final internal exposure concentration following a sudden external exposure of the gas (step function).

6.2 Calculation conditions

Calculations are performed for humans, using the airway geometry for the "standard man", see chapter 1, and using the respiration conditions for exercise at 50W, identical to conditions for the evaluation study, sections 5.1 and 5.2, although nose breathing is simulated in this case.

For ammonia and sulphur-dioxide, calculations are also performed for rats, using the geometry and conditions described in chapter 2.

6.3 Ammonia (NH_3)

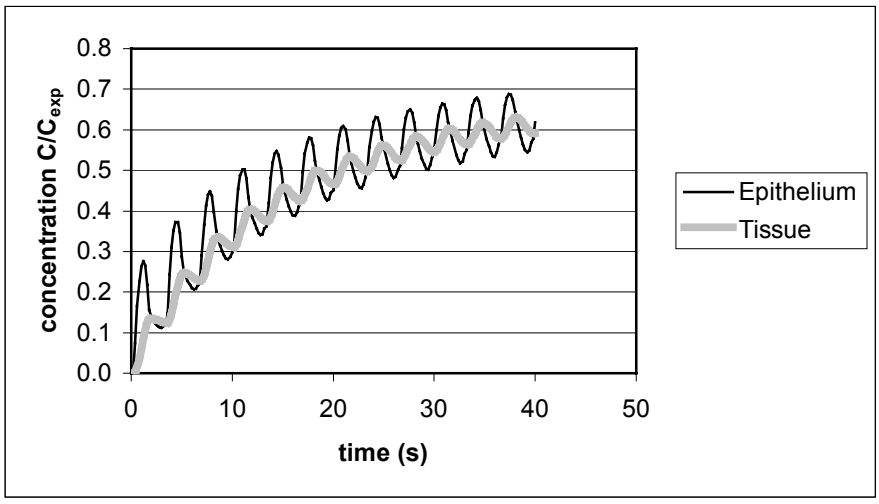

Figure 6.1. Example of the internal dose. The Figure shows the concentration in the epithelium and tissue of the 1st level bronchioles following a stepwise exposure to ammonia. The concentration in the epithelium is in almost instantaneous equilibrium with the lining and air. Concentrations are expressed as mass concentration, divided by the exposure mass concentration in the air.

Calculations were performed following a step function exposure starting at time t=0, which is also the time for a new inhalation. The calculation duration is 40 s for the human and 60 s for the rat. The concentrations in the airways, the lining, the epithelium as well as in the tissue at the lower airway elements follow a fluctuating pattern corresponding to the respiration pattern, with an increasing trend as the whole airway system absorbs the substance and reaches a state of equilibrium, see e.g. Figure 6.1. In the upper airway, the tissue is thicker, and

the concentration in the tissue does not follow the respiration pattern, as in Figure 5.4.

We estimate the asymptotic concentration C_∞ for the internal exposure of the lining, epithelium, and tissue together with the time scale τ assuming a first order response to the step function exposure:

$$C_{internal\ exposure}(t) = C_\infty\left(1 - \exp(-t/\tau)\right). \qquad \textit{Equation 6.1}$$

We do this both for the maximum concentrations (i.e. during inhalation) and the minimum concentrations (during exhalation). It appears that a first order response is a reasonable assumption for most of the situations, although it is clear in some occasions, that there is more than one time scale, e.g. the time scale of the layer itself and the time scale of the whole airway system.

Results for the human airway system are presented in Table 6.2. The concentration in the thin lining layers in the upper airways (nares and trachea) adjusts rapidly to the external exposure. The time scale for the epithelium in the nares is slightly more than the estimated time scales for acetone (see Table 5.3). Timescales for tissue in the nares and trachea couldn't be estimated on the basis of a 40 s. calculation, in this case estimates for acetone suggests values in the order of 200 s. Although the lining and epithelium are thinner for the lower airways, the time scales are larger. This is typical for very soluble gases. The uptake of gas in the upper airways is so effective, that it takes some time before the gas penetrates deeper in the airways. For the bronchioles at level 1 and the terminal bronchioles, the time scales for lining, epithelium and tissue are almost the same, suggesting that these time scales are dominated by processes involving the whole airway system.

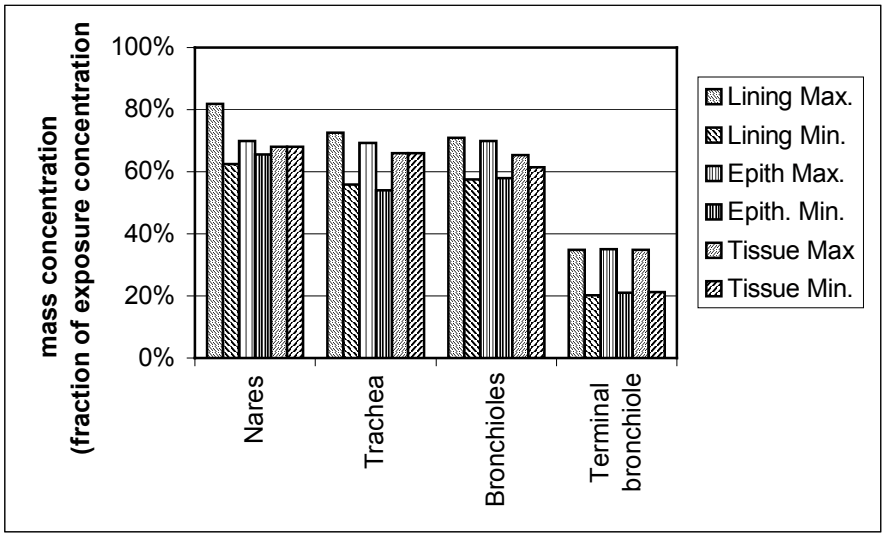

Figure 6.2. Asymptotic values of mass concentration in the human airways following a step function exposure to ammonia. Concentrations are expressed as percentages of the equilibrium concentration in the layers corresponding to the external exposure concentration.

The asymptotic concentrations, also shown in Figure 6.2, are well below 100%, decreasing towards the lower part of the airways. The gas doesn't penetrate significantly deeper than the first respiratory bronchioles, where is effectively removed by the blood.

Another characteristic of soluble gases is that the difference between maximum and minimum concentrations is relatively small, due to the buffering ef-

fect of the gas absorbed and desorbed by the walls during inhalation and exhalation, respectively.

Table 6.2. Estimates of time scales and asymptotic values of the concentrations in the wall layers of human airway elements for ammonia. Concentrations are expressed as percentages of the equilibrium concentration in the layers corresponding to the external exposure concentration.

		Lining		Epithelium		Tissue	
		time scale (s)	Asymp-tote	time scale (s)	Asymp-tote	time scale (s)	Asymp-tote
Nares	min	7.6	62%	6.5	65%		
	average					>70	ca 67%
	max	1	82%	3.6	70%		
Trachea	min	12	56%	12	54%		
	average					>100	ca 66%
	max	1.3	73%	1.9	69%		
Bronchioles level 1	min	14.8	58%	12.7	58%	15.1	61%
	average						
	max	7.3	71%	7.9	70%	12.5	65%
Terminal bronchiole	min	20	20%	30	21%	32	21%
	average						
	max	23	35%	24	35%	24	35%

In case of ammonia, we have some data on concentration in exhaled air from experiments with humans (Silverman et al., 1949). During these experiments, seven male adults were exposed to anhydrous ammonia at 500 ppm during 30 min. Respiration rate, ventilation rate and concentration in exhaled air were measured and some other physiological and subjective reactions registered. It was observed that ventilation rate and respiration rate increased upon exposure, and changed cyclically during the exposure period. The concentration in exhaled air changed during these cycles. Finally, the concentration in exhaled air reached on average 77% of the exposure concentration. This equilibrium level was reached after 10 to 25 min., though responses to changes in expiration patterns were apparently faster. The recovery time to reach base level was between 3 and 8 min. It should be noted that from the description of the experiment it is unclear whether Silverman et al. could resolve concentration measurements at less than 3 min. The results are compared with the present results in Figure 6.3. The time scale that is calculated by the present model (first order response time) is about 17 s, thus considerably shorter than reported by Silverman et al. The predicted equilibrium concentration in exhaled air (about 65%) is not in contradiction with the experimental results.

Silverman et al. observed that the exhaled air contained some undetermined amines. A part of the increased buffering of ammonia can be due to chemical reactions, increasing the response time. The present model does not include chemical reactions, and supposes 100% reversible absorption and desorption from the lining, epithelium and tissue. Neither accounts the model for the significant physiological effects, i.e. the increase of ventilation rate by 50% to 250% at these relatively high exposure concentrations.

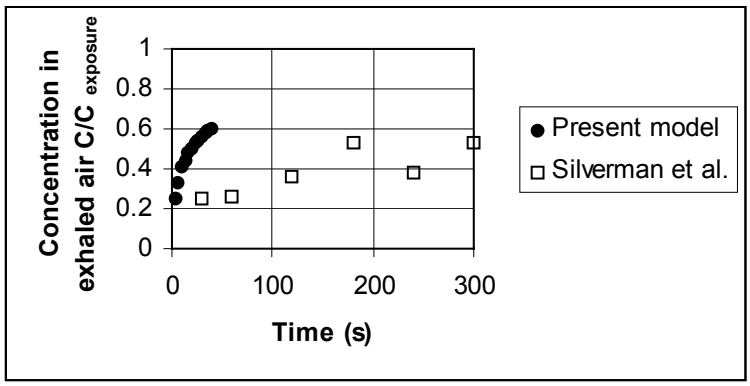

Figure 6.3. Comparison of present model results with experiments from Silverman et al.. The graph shows the averaged concentration in exhaled air (fraction of concentration in exposed air). Results for the first 5 min. for Silverman's subject No. 7 are included.

The model calculation results for exposure of a rats with ammonia are presented in Figure 6.4 and Table 6.3. Surprisingly enough, for ammonia the time scales in a small rat are larger than for a human being. For that reason, the calculation period was 60 s in this case. Even though, it was not possible to estimate the asymptotic internal exposures for elements deeper than the nose region from a 60 s. record, having time scales longer than 100 s, say.

Table 6.3. Estimates of time scales and asymptotic values of the concentrations in the wall layers of rat airway elements for ammonia. Concentrations are expressed as percentages of the equilibrium concentration in the layers corresponding to the external exposure concentration.

		Lining		Epithelium		Tissue	
		time scale (s)	Asymp-tote	time scale (s)	Asymp-tote	time scale (s)	Asymp-tote
Nares	min	7.3	72%	6.4	76%	9.1	84%
	average						
	max	2	83%	4.7	79%		
Ethmoturbi-nate region	min	17	60%	23	60%	39	61%
	average						
	max	22	61%	21	61%		

Part of the explanation is that the surface area of the rat's nose is larger than the human's nose's surface. Ammonia is therefore more effectively removed by the rat's nose, and the following slow diffusion in the nose's tissue causes the whole rat airway system to respond slowly. The fact that the surface-to-volume ratio of all airway elements in the rat is larger than in humans (a logical consequence of the smaller size of the rat) has the same effect. Anyway, over a 40 to 60 s period of exposure, concentrations in humans will be close to final, asymptotic values (except for the thicker tissue layers in the upper airways), while in rats, very low, but steadily rising concentrations are found from the nasopharynx downwards. The slow penetration of ammonia into the rat lung is also illustrated by the fact that after 60 s, only 5% of the total net mass of ammonia inhaled is absorbed by the blood, while in humans this is already 20% after 40 s.

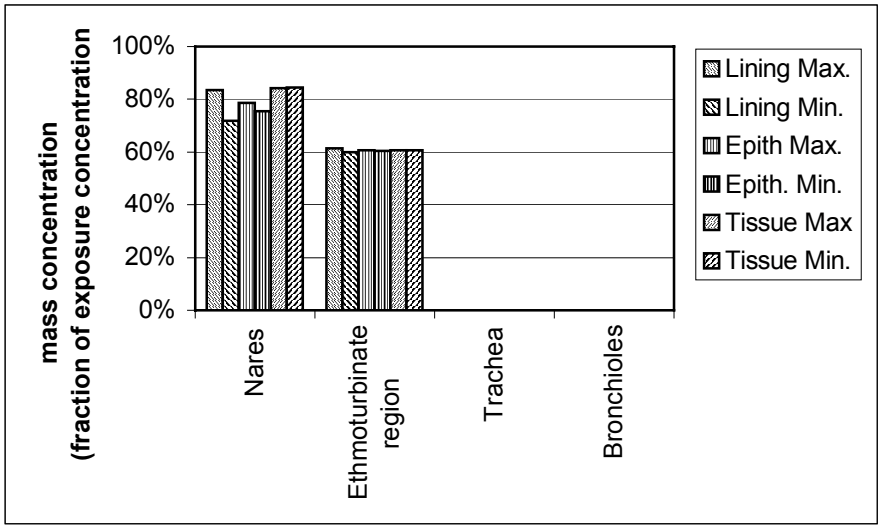

Figure 6.4. Asymptotic values of mass concentration in the rat airways following a step function exposure to ammonia. Concentrations are expressed as percentages of the equilibrium concentration in the layers corresponding to the external exposure concentration.

6.4 Sulphur-dioxide (SO_2)

For SO_2 the same calculations have been performed as for ammonia, though the calculation period was 40 s both for the human and rat case. SO_2 has a partition coefficient of 42 (based on mass concentrations) and the equilibrium concentration in the aqueous phase is therefore about a factor 50 lower than for ammonia. Still, absorption of sulphur-dioxide plays a role in determining the pattern of the internal dose in the airways.

Results for the human system are presented in Table 6.4 and Figure 6.5. From Equation 5.1 it follows that the average alveolar concentration of SO_2 should be about 10% of the exposure concentration. This is in agreement with the minimum concentration in the alveolar duct and the terminal bronchiole. The absorption of gas in the upper airways down to the terminal bronchiole is low: the maximum concentrations are only reduced a few percent (at the terminal bronchiole). The minimum concentration at the nose shows some effects of desorption of gas during exhalation, but is mainly due to the inertia of the diffusion process. Time scales are small (1 – 2 s) and fairly uniform throughout the whole airway system, except for the time scales of the thick tissue layers in the upper airways. This is also caused by the fact that the alveolar equilibrium concentration is low, and this equilibrium stage is reached almost instantaneously. This means that maximum exposure of the airway walls (again with exception of the tissue layers at the upper airways) is already reached within a single breath.

Table 6.5 and Figure 6.6 show the results for a rat. In this case, SO_2 behaves more like a soluble gas. In a rat, absorption and desorption during inhalation and exhalation have a clear effect on the concentration pattern, and unlike in the human case, the concentration decreases gradually towards the lower airway elements. Time scales are very similar to those in humans in absolute terms, but it should be noticed, that in rats equilibrium is reached after at least 5-6 breath cycles, contrary to the human case.

Table 6.4. Estimates of time scales and asymptotic values of the concentrations in the wall layers of human airway elements for SO_2. Concentrations are expressed as percentages of the equilibrium concentration in the layers corresponding to the external exposure concentration.

		Lining		Epithelium		Tissue	
		time scale (s)	Asymp-tote	time scale (s)	Asymp-tote	time scale (s)	Asymp-tote
Nares	min	1.5	33%	1.9	51%		
	average					67	75%
	max	0.4	91%	0.9	87%		
Trachea	min	2.3	23%	2.6	24%		
	average					57	68%
	max	0.3	95%	0.3	91%		
Bronchi-oles level 1	min	1.4	27%	1.4	29%	1.6	44%
	average						
	max	0.5	92%	0.6	91%	1	84%
Terminal bronchiole	min	1.7	12%	1.6	13%	1.7	13%
	average						
	max	0.4	96%	0.4	96%	0.4	96%
Alveolar duct 1	min	2	8%	2	8%	2	8%
	average						
	max	0.5	63%	0.5	63%	0.5	63%

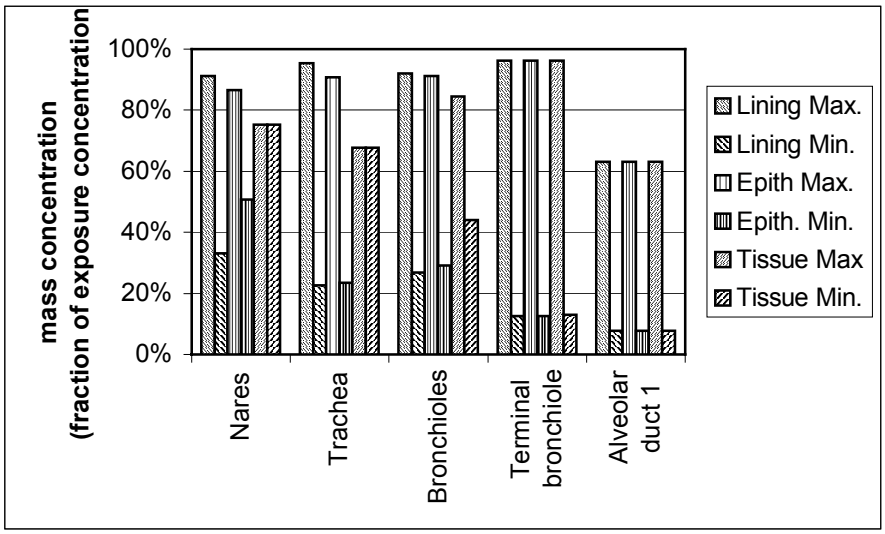

Figure 6.5. Asymptotic values of mass concentration in the human airways following a step function exposure to SO_2. Concentrations are expressed as percentages of the equilibrium concentration in the layers corresponding to the external exposure concentration.

Table 6.5. Estimates of time scales and asymptotic values of the concentrations in the wall layers of rat airway elements for SO_2. Concentrations are expressed as percentages of the equilibrium concentration in the layers corresponding to the external exposure concentration.

		Lining		Epithelium		Tissue	
		time scale (s)	Asymp-tote	time scale (s)	Asymp-tote	time scale (s)	Asymp-tote
Nares	min	2	76%	2	76%	3	91%
	average						
	max	0.1	94%	0.1	94%		
Trachea	min	2.7	60%	3.1	66%	4	70%
	average						
	max	2.4	76%	2.9	73%	4	74%
Bronchi-oles level 1	min	1.5	39%	1.5	42%	1.5	53%
	average						
	max	0.9	77%	1	74%	1.4	62%
Terminal bronchiole	min	1.6	19%	1.6	22%	1.6	28%
	average						
	max	0.9	58%	1.4	55%	1.5	49%
Alveolar duct 1	min	1.8	8%	1.8	8%	1.8	8%
	average						
	max	1.6	25%	1.6	25%	1.6	25%

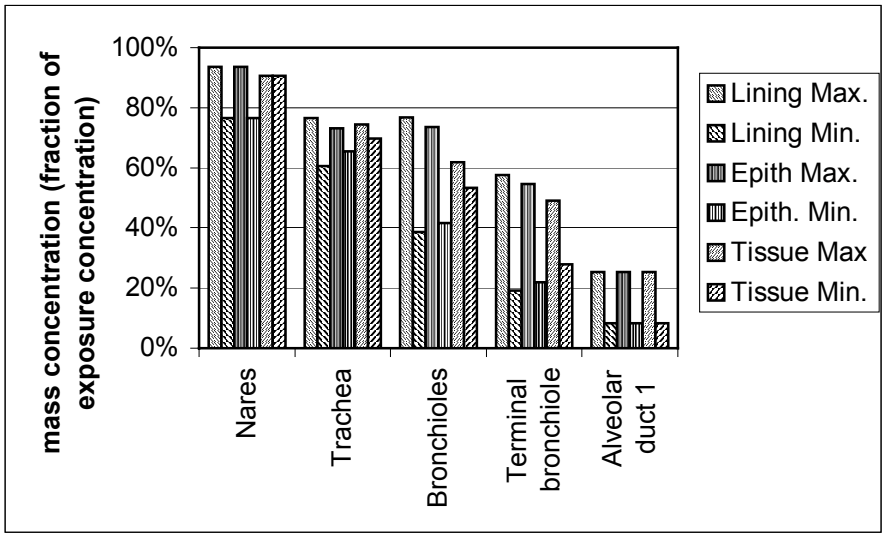

Figure 6.6. Asymptotic values of mass concentration in the rat airways following a step function exposure to SO_2. Concentrations are expressed as percentages of the equilibrium concentration in the layers corresponding to the external exposure concentration.

6.5 Hydrogen-sulphide (H_2S)

Hydrogen-sulphide is an example of a hardly soluble substance, with a partition coefficient of about 410. For this substance, only results for the human case are presented. It is expected that the situation in rats will be very similar. Results are included in Table 6.6 and Figure 6.7.

According to Equation 5.1, the average alveolar concentration is about 51%. This is in very good agreement with the minimum concentrations (i.e. concentrations at the end of exhalation) throughout the whole airway system. No significant absorption or desorption occurs in the non-alveolated part of the airways, so concentrations during inhalation in this part are almost 100%, deviations are due to the inertia of diffusion. Overall time scales are slightly higher than for SO_2, which is caused by the fact that it takes several breaths before the total lung volume is replaced by air at the exposure concentration. This depends on the ratio between the tidal volume and the functional reference capacity (FRC). At the conditions used here (exercise at 50 W), after 2 breaths, i.e. 6-7 s, the lung concentration reaches 49% if alveolar uptake by the blood is neglected. This explains the time scales for the minimum concentrations (i.e. concentrations at the end of exhalation) very well.

Table 6.6. Estimates of time scales and asymptotic values of the concentrations in the wall layers of human airway elements for H_2S. Concentrations are expressed as percentages of the equilibrium concentration in the layers corresponding to the external exposure concentration.

		Lining		Epithelium		Tissue	
		time scale (s)	Asymp-tote	time scale (s)	Asymp-tote	time scale (s)	Asymp-tote
Nares	min	5.6	53%	3.5	63%		
	average					>100	ca. 74%
	max	0.4	97%	1	84%		
Trachea	min	6.2	49%	6.3	50%		
	average					>100	ca. 72%
	max	0.3	98%	0.3	94%		
Bronchi-oles level 1	min	6	50%	5.8	51%	4.4	64%
	average						
	max	0.3	99%	0.5	98%	1.5	86%
Terminal bronchiole	min	6.2	49%	6.2	49%	6.3	50%
	average						
	max	0.2	99%	0.2	99%	0.3	98%
Alveolar duct 1	min	6.5	48%	6.5	48%	6.5	48%
	average						
	max	1.5	67%	1.5	67%	1.5	67%

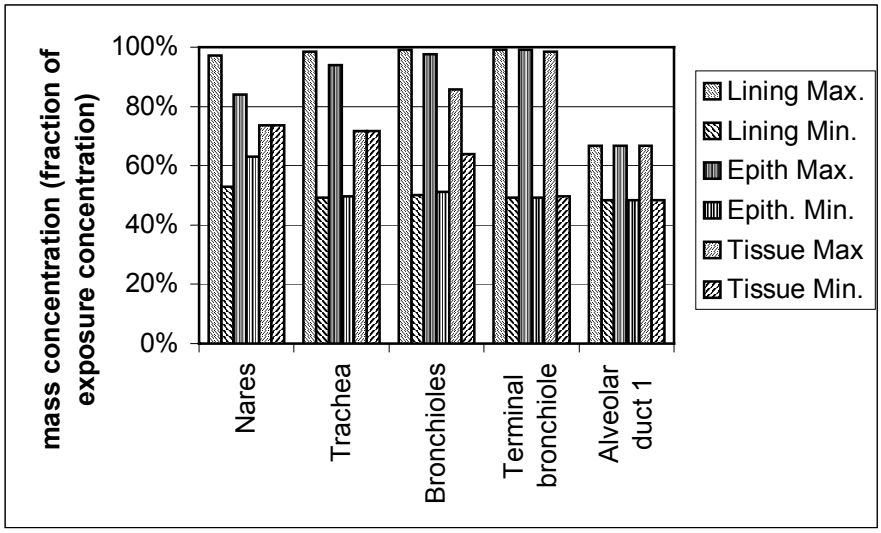

Figure 6.7. Asymptotic values of mass concentration in the human airways following a step function exposure to H_2S. Concentrations are expressed as percentages of the equilibrium concentration in the layers corresponding to the external exposure concentration.

6.6 Distribution of mass

Another comparison of the three substances can be made by looking at the distribution of the mass between the different compartments (air, lining, epithelium, tissue and blood). These distributions are shown in Figure 6.8. The Figure shows how fast the airway system reaches an equilibrium state. In an equilibrium state, the amount of mass present in lining, epithelium and tissue, as well as in the air in the lung, are constant with time (apart from the fluctuations related to the respiration pattern). Then the increase in the total net amount of mass in the airways (inhaled minus exhaled) is equal to the increase of mass in the blood, i.e. these two lines will have the same slope. It can be seen that in the case of ammonia, equilibrium is not reached within 40 s. The amount of mass in the tissue is still raising, and only a small fraction of the ammonia is absorbed by the blood. In case of sulphur-dioxide, equilibrium is obtained very fast. In case of hydrogen-sulphide, it takes a bit longer. In this case, the amount of mass in the air is also shown. Contrary to the better soluble ammonia and sulphur dioxide, a considerable fraction is present in the air in the lungs. This is because in this case the gas penetrates into the deepest alveoli, and the alveolar region has a considerable volume, much larger than the volume of the upper airways (see Table 1.3).

Note that the net uptake of the three different gases is (almost) equal, even though the partition coefficient varies more than a factor 400. Under equilibrium conditions, this uptake depends only on the ratio of the ventilation rate and the cardiac output.

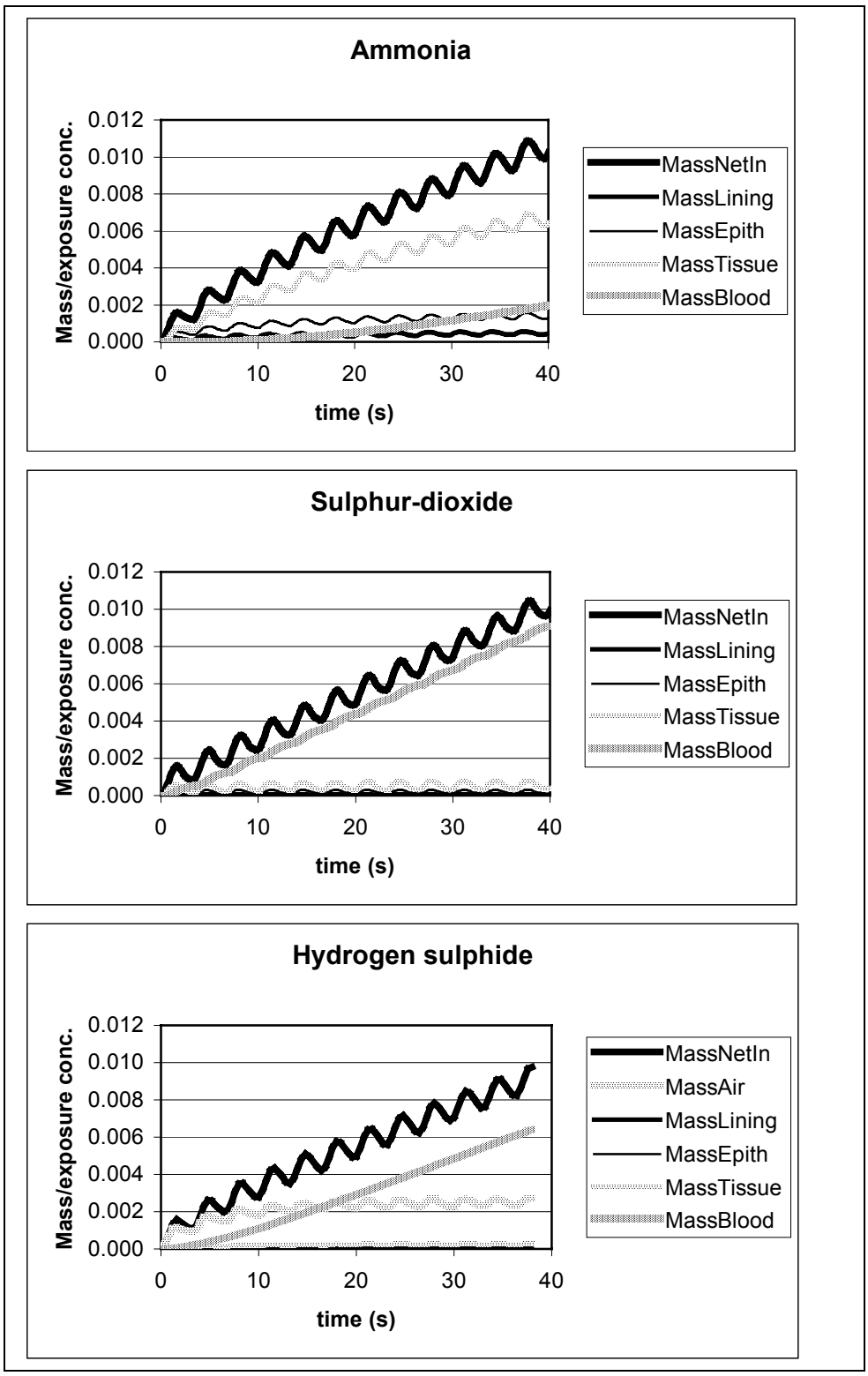

Figure 6.8. Distribution of the net inhaled mass of gas in the human airways. MassNetIn is the sum of inhaled and exhaled gas.

7 Exposure to fluctuating concentrations

In this chapter we will apply the findings from the previous chapters to the practical situation of exposure to fluctuating concentrations. We will apply theory from control systems analysis to two extreme though relevant situations, i.e. the exposure to a single, (short) finite duration pulse, and exposure to a periodic time series of concentration. Real exposures, e.g. in atmospheric clouds of toxic material, will be in the form of a stochastical time series, but it will contain features from both types of idealised exposure.

7.1 Response to single concentration pulses

Using the information provided by the asymptotic internal exposure concentrations included in Table 6.2, Table 6.3, Table 6.4, Table 6.5, and Table 6.6 together with the time constants τ in these tables, it is possible to construct the response of the internal exposure concentration (i.e. the concentration in a wall layer of a selected element in the airways) from Equation 6.1 directly. For exposure to a constant concentration C starting at time t_{start} and ending at time t_{end}, the response will be:

$$C_{internal\ exposure}(t) = KC\left(1-\exp(-(t-t_{start})/\tau)\right) \text{ for } t_{start}<t\leq t_{end}$$
$$C_{internal\ exposure}(t) = KC\left(\exp(-(t-t_{end})/\tau)-\exp(-(t-t_{start})/\tau)\right) \text{ for } t>t_{end}.$$

Equation 7.1

Here, the asymptotic internal exposure concentrations included in Table 6.2, Table 6.3, Table 6.4, Table 6.5, and Table 6.6 are included as the amplification factors *K*. If absolute concentrations in the wall layers are required, the values need to be divided by the partition coefficient between the air and the wall layer in question.

7.2 Frequency response using Fourier decomposition

In chapter 6, the response of the human and rat airways to a step function exposure is analysed. This information can be used to predict the internal dose in the airways in response to a fluctuating exposure concentration. Therefore we use principles from time series and control system analysis.

Any periodic time series, and therefore any periodic series of exposure concentration, can be decomposed into a number of harmonic series (Fourier decomposition):

$$C_{exposure}(t) = a_0 + \sum_{n=1}^{\infty} a_n \cos(2\pi n f t) + \sum_{n=1}^{\infty} b_n \sin(2\pi n f t) \qquad \textit{Equation 7.2}$$

Here, *f* is the lowest frequency in the periodic series. This idea can be extended to *any* (i.e. non-periodic, like step functions or single pulses) time series or sig-

nal, in that case the discrete summations turn into integrals over an infinite number of frequencies. We then speak about Fourier integrals, which in its simplest form can be written as:

$$C_{exposure}(t) = 2\int_0^\infty [D(f)\cos(2\pi ft + \Phi(f))]df \qquad \textit{Equation 7.3}$$

Here, D(f) represents the amplitude corresponding to frequency f, and Φ(f) the phase shift at this frequency.

The asymptotic internal exposure concentrations included in Table 6.2, Table 6.3, Table 6.4, Table 6.5, and Table 6.6 can be considered to be static amplification factors *K* of the dynamic response function of the airway element in question. The same tables provide the time constants τ for these functions. The response function consists of two parts, first the amplification of the amplitude α(f), and the phase shift of the resulting series compared to the external exposure series ϕ(f):

$$\alpha(f) = \frac{K}{\sqrt{\frac{f^2}{4\pi^2}\tau^2 + 1}}$$
$$\phi(f) = -\arctan(2\pi f\tau) \qquad \textit{Equation 7.4}$$

Normally, α(f) will be sufficient to obtain an estimate of the final level of the internal exposure concentration for a given external exposure signal with an overall frequency f. But for more complex situations this response function can be applied to a Fourier transformed signal in order to determine the internal exposure concentration. For the Fourier transform of the internal exposure can be written:

$$D_{internal}(f) = \alpha(f)D(f)$$
$$\Phi_{internal}(f) = \Phi(f) + \phi(f) \qquad \textit{Equation 7.5}$$

Now the series of the internal exposure concentration can be obtained from inverse Fourier transform of $D_{internal}$ and $\Phi_{internal}$. In the majority of cases, this will be quite a tedious task, requiring numerical procedures.

7.3 Interaction with the respiration pattern

The theory provided in the previous two sections ignores the fact that the airways only have an intake of the externally exposed gas during inhalation. Sampling by the airways is, so to speak, intermittent. Therefore, the above methodology can only be applied for concentration pulses with a length of at least one respiration cycle or for time series when the highest frequency is less than half of the respiration frequency.

For a single pulse shorter than the length of a respiration cycle, the best procedure is to replace it by an *ensemble averaged* pulse, lasting for the duration of the respiration cycle, and adjusting the concentration as to maintain the dose.

For periodic exposures, it is not so easy to provide a way of handling exposures that are dominated by frequencies less than twice the respiration frequency. This is probably an academic problem, as most practical exposures will

be stochastic, and high frequency variations should be filtered out. But just to show the consequences, imagine that the exposure time series has exactly the same frequency as the respiration. If inhalation and high exposure concentrations are in phase, the subject will perceive the exposure as being a constant exposure, not noticing the low concentrations during exhalation. If inhalation is out of phase with the high concentrations, the subject will not perceive an exposure at all.

8 Application to atmospheric gas clouds

8.1 Atmospheric data

In this chapter an atmospheric plume from a continuous release of ammonia is considered as an example of real data. Generally the concentration inside a plume is a highly fluctuating quantity. This has several causes. The mixing of the plume with the surrounding air is a stochastic process driven by turbulence. Eddies that are roughly the size of the diameter of the plume are responsible for most of the mixing, while they, at the same time, constantly create concentration differences as air is 'stirred' into the cloud. . Plumes never reach a 'well mixed' state but continue to undergo mixing with the air that surrounds it at any point downwind of the source.

Eddies that are small compared to the plume diameter have little effect except to even out concentrations over small distances. Eddies larger than the plume diameter tend to create meandering rather than mixing, because they move the plume as a whole without mixing. As a result the concentration a fixed downwind position is characterised by fluctuations caused by in-plume inhomogeneities and intermittency created by the meandering. The intermittency is caused by the fact that the observation point is sometimes inside, sometimes outside the plume.

Figure 8.1a shows an example of a concentration time series measured in an atmospheric plume from a ground source. The measurements were taken during trial023 of the FLADIS experiment (Nielsen & Ott, 1996). Detailed release conditions can also be found in the REDIPHEM database (Nielsen & Ott, 1995). The data shown were sampled at a rate of 20 measurements per second with an UVIC® sensor located 150m downwind of an ammonia source. The UVIC is a very fast instrument, fast enough to justify the sampling rate, and the data can be regarded as virtually free of instrumental effects. The figure shows 200 seconds out of a total length of 1200 seconds. The example is typical and representative for other substances than ammonia. It also has scaling properties. Multiplication by a constant factor scales the signal to match other source strengths. A rescaling of time axis should have the same effect as changing the downwind position. Thus characteristic time scales, e.g. the duration of zero concentration periods, increase with downwind distance.

The wild fluctuations are the most prominent feature of the signal. It alternates between periods with bursts of sharp peaks and periods of complete absence of the plume. A very large range of concentrations is released. Reducing such complexity to a few discrete statistics might lead to severe loss of information. The mean value is, for example, looses its significance as actual values are likely to be either much higher or much lower than the mean. It may therefore seem more relevant to base averages exclusively on periods where the signal is

non-zero, so-called conditional sampling. For the present example the conditional average concentrations is about 2 times higher than the unconditional average. An alternative method, the so-called moving frame method, utilises a cross-plume array of sensors to define concentrations relative to the instantaneous plume centre. From this one can form e.g. the average concentration at the centre of the plume (which is generally moving around). This mean value is generally larger than the conditional average. It is important to realise that different data analyses yield quite different averages.

The probability density function (pdf), i.e. the frequency of occurrence of a given concentration value, represents somewhat more complete information. Although the pdf contains more information than just an average value, it does not cover all aspects of the fluctuations. For example it is likely important whether a certain concentration level occurs frequently and for short periods of time, or it occurs rarely but for long periods. The pdf does not distinguish between these two behaviours. A more complete description therefore also has to cover the duration aspect. Statistics the quantify the durations of the periods with zero concentration might also be of interest in case they allow for some kind of recovery.

8.2 Time averaging

Physiological effects are caused by concentrations within the body. These result from concentrations in the air, but air concentrations are not the main parameter, because the respiratory system acts as a filter. The airway model described in the previous chapters can be regarded as specifying a set of filters characterising the build-up of concentrations in various parts of the respiratory system as a response to concentrations in the air. The response analysis of the lung model shows that characteristic response times depend much on the location within the respiratory system and also differ for different substances. From chapter 6 it appears that time scales for the reaching final internal exposure concentrations vary between about 1 s for lining and epithelium up to more than 100 s for tissue layers, depending on the substance and the site in the lung. Therefore we show the effect of averaging time scales of 1, 10, 100 and 1000 s.

In order to illustrate the effect of time averaging simple first order filters have been applied to the measured time series of Figure 8.1, curve a. Filtered signals are shown in curves b-d for three different averaging times: 1s, 10s and 100s. A first order filter is equivalent to putting the sensor into a ventilated, well mixed compartment, where the averaging time equals the volume divided by the ventilation rate. The main feature of the filtered signals is the reduction of the concentration range due to smearing of peaks and 'filling' of the periods with zero concentrations. The main effect of averaging is to make the curved flatter and reduce the concentration range. An averaging time of 100s almost completely smears out the peaks.

All sensors have a finite response time. For most commonly used sensors it is much longer than in the example shown here. Therefore time averaging enters the problem also in this way. If a measured time series is to be used to assess toxic effects, the instrumental averaging time must match the physiological averaging time.

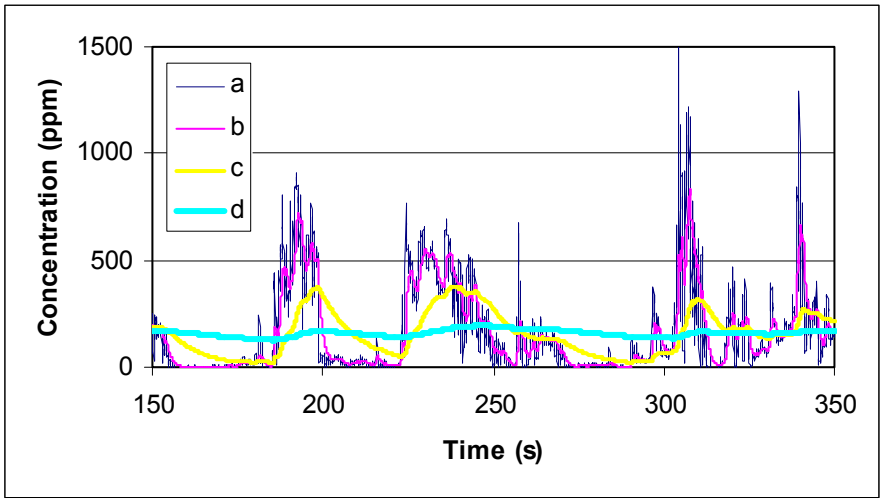

Figure 8.1. A concentration time measured in a plume. a: raw data, b:1s filter, c: 10s filter, d:100s filter.

8.3 Dispersion models

Toxic effects are often assessed from model results rather than from actual measured data. Models can only predict reproducible features of dispersion, in other words statistics, and in practice only mean concentrations are available. Models of the dispersion from a constant rate source, e.g. CFD models or a box models, are typically expressed in terms of quantities averaged over an ensemble of realisations, which in turn is assumed to be equal to a time average over an infinite averaging time. In most models the large scale eddies, which are responsible for the meandering that creates the pauses in the concentration signal, are not explicitly accounted for, which leaves doubt as to the extent to which meandering can be considered part of the model. Therefore it is often unclear which type of average apply to concentrations predicted by models. In most cases the only hint is the data analyses applied to the data that are used to tune model parameters. In any event a model prediction would resemble the 100s average more than the shorter averages.

8.4 Toxic effects

Toxicological experiments are often interpreted in terms of probit functions, and probit functions are often used in conjunction with model results to assess toxic effects. In the following the implication of time averaging on probits is investigated.

We refer to the parallel report on the TEARHS project by Arts et al. (2000). In a typical animal experiment rats are exposed to a constant concentration C for a certain period of time T. The mortality rate is estimated for a number of combinations of C and T and an experimental probit function Y(C,T) is fitted to the data. The following functional form is used for the fit

$$Y = A + B \ln(C^n T)$$

where A, B and n are substance specific constants. The quantity $D=C^nT$ is referred to as the dose. The question is how Y, or D, should be estimated from an experimental time series.

For this purpose the experimental time series of Figure 8.1a is taken as an example. We will allow the time series to represent an ammonia release (as it actually does) or let represent one of the substances that have been investigated in

the present study. For non-constant concentrations we follow convention and replace C^nT by $\int c^n(t)\,dt$. This is not the only possible generalisation. For example C could be taken as the conditional average and T could be adjusted down in order only to take periods with non-zero concentrations into account. It is also necessary to specify what in meant by c(t). We could take c(t) to be the concentration in the air or, perhaps better, we could choose a suitably filtered concentration. Whenever model results are used to evaluate D some kind of filtering is involved, hence practice shows that averaging c(t) is an option.

Time series corresponding to larger or smaller release rates can be emulated by a simple rescaling of the concentration. Replacing c(t) by k c(t), where k is a constant, is equivalent to replacing A with the value A' = A + n B ln(k). It is therefore merely a matter of adding a constant to Y. In a similar fashion a rescaling of the time axis, for the purpose of emulating a different downwind distance, just shifts Y by a constant amount. The uncertainty of the probit Y, introduced by any lack of knowledge of the proper choice of averaging time, is therefore independent of both the release rate and the distance from the source.

Table 8.1 shows probits evaluated for the raw signal as well as for averaging times of 1s, 10s, 100s and 1000s. The exponent n in the expression for the dose is taken from Arts et al. (2000). The probit levels are adjusted arbitrarily so that Y=5 for 10s averaging time.

Table 8.1. Probits evaluated from an experimental time series after applying three different first order filters. The 2nd column lists the exponent in the expression for the dose for each substance.

Substance	n	Raw data	$T_{average}$ =1s	$T_{average}$ =10s	$T_{average}$ =100s	$T_{average}$ =1000s
$COCl_2$	0.789	4.5	4.6	5	6.7	7.1
Cl_2	1.040	5.1	5	5	4.9	4.7
HCl	1.592	6.2	5.8	5	3.9	1.4
NH_3	2.012	6.7	6.2	5	3.5	0.4
H_2S	8.291	10.5	8.5	5	-0.4	-6.1

Table 8.2. Predicted mortalities (%) corresponding to the probits of Table 8.1.

Substance	Raw data	$T_{average}$=1s	$T_{average}$=10s	$T_{average}$ =100s	$T_{average}$ =1000s
$COCl_2$	31	34	50	95.5	98.2
Cl_2	54	50	50	46	38
HCl	88	79	50	14	0.016
NH_3	95.5	88	50	6.7	0.0003
H_2S	100	99.98	50	3.33E-06	0.00E+00

There is little difference between the results for the raw data and for the data filtered with an averaging time of 1s. This indicates that 1-second averages are sufficiently resolved. For larger averaging times the differences are more pronounced, and the tendency increases rapidly as the exponent n increases. In Table 8.2 the corresponding mortalities are listed. For phosgene and chlorine, for which $n \approx 1$, averaging has little effect. For HCl and ammonia predictions vary by an order of magnitude. For H_2S the effect of averaging is so enormous that the even the slightest adjustment of the averaging time change the predicted mortality completely.

The concentration-time-fatality relations by Arts et al. are obtained using rats being exposed to a constant concentration during at least 5 minutes. Arts et al.

recommend not to use these relations for exposures lasting less than one minute: in that case it is suggested to use n=∞. Neither does Arts et al. present recommendations how to apply these relationships to fluctuating concentrations.

We have chosen to apply Arts et al.'s recommendation for short duration exposures for fluctuating concentrations as well. In this way we come to the following procedure: As before a first order filter was applied to the raw signal. Then the filtered series subsequently was divided into 1-minute intervals and the maximum was determined for each interval, and the dose was calculated using the maximum concentration for each interval.

Table 8.3 shows mortalities evaluated following this method. Probit values are scaled in such a way, that mortalities are comparable with those presented in Table 8.2. This method yields considerably higher mortalities than the other method, particularly for small averaging times. It is evident that averaging has a very large impact on the predicted mortalities.

Table 8.3. Predicted mortalities (%) based on 1-minute maxima of filtered concentrations.

Substance	Raw data	$T_{average}$=1s	$T_{average}$=10s	$T_{average}$ =100s	$T_{average}$ =1000s
$COCl_2$	100	100	99.85	83	95
Cl_2	99.9998	99.97	95.2	61	42
HCl	100	100	99.89	34	0.038
NH_3	100	100	99.5	19	0.001
H_2S	100	100	56.5	1.65E-05	0.00E+00

If the data is processed in this way, we observe a very important effect of averaging time, i.e. the response time scales of the exposed lining and tissue layers in the airways, on the assessment of toxicity. Even for chlorine, for which one would expect no effect of concentration fluctuations, as the exponent is almost equal to one, enormous differences in the assessment occur. Hydrogen sulphide shows the most extreme effect. For this substance there exists effectively a kind of concentration limit irrespective of the exposure duration beyond the subject dies. This behaviour is assessed (with rats) down to exposures of 5 minutes. The essential question is, whether this behaviour can be extrapolated down to extremely short exposures, e.g. during a few seconds. On the contrary, note the increase of predicted fatality for phosgene if the averaging time is raised from 100 s to 1000 s. Apparently low concentrations periods still present when averaging over 100 s reduce the toxic dose compared to the 1000 s-averaged concentrations.

8.5 Discussion

In this example we have applied two methods of assessing toxic effects to experimentally observed time series of concentration fluctuations. These methods are logical extrapolations using information on the toxic effects of constant exposures over finite periods. It should be stressed that there is no information available that contains guidance how to use concentration-time-fatality relationships of Probit-functions in combination with fluctuating concentrations, e.g. considering recovery between peak concentrations. The recommendation based on one-minute maximum concentrations (after filtering using the averaging time appropriate for the airway element of interest) is a conservative approach. It is especially conservative for substances with relatively small exponents (like chlorine and phosgene), while simply extrapolating the concentration-time-

fatality relationships to small time scales may be underestimating the toxic effects for some substances.

Either way, neglecting concentration fluctuations on the scale of 10 seconds where this is shown to be a relevant time scale (see chapter 6), will lead to an underprediction of toxic effects for substances that appear to have an exponent larger than 1 in the concentration-time-fatality relationship.

9 Hydrolysis and degradation of phosgene in airway tissue

9.1 Introduction and scope

Phosgene ($COCl_2$) is a very common and important intermediate in chemical industries and is used in many different applications, for instance in the production of isocyanates, which are intermediates in polyuretane manufacturing. Nowadays about 700000 t phosgene per year are used in the chemical industries. Phosgene is also produced by heating and combustion of chlorinated hydrocarbons or by photochemical reactions of these compounds. Examples are the use of tetrachloromethane containing extinguishers, which can produce significant phosgene concentrations under usage and welding of components not correctly cleaned with chlorinated solvents. (Roth-Weller, 1999). Phosgene is listed on Schedule 3 of the Chemical Weapons Convention, as it is very toxic. In the following, phosgene's toxic effects and its reactivity towards water are briefly reviewed. Based on the findings a simple kinetic model is developed using a compartment approach that reduces the time and distance dependent problem into a time dependent model.

9.2 Physical chemical properties

Phosgene is a colourless gas or a clear to yellow liquid, registered under the CAS no. 75-44-5 and the DOT no. UN 1076. The odour threshold is from about 0.4 to about 1.5 ppm (Schneider and Diller). The odour, which can only be detected briefly at initial exposure times, is reported to be of mouldy hay, but may be strong, stifling and unpleasant at high concentrations (Hardy). The solubility of phosgene is only slightly in cold water and at higher temperatures it hydrolyses rapidly. The following estimations are found in the SRC PhysProp web based database[2] together with the citation of the original literature:

- The octanol-water partition coefficient is calculated to log P_{OW} = -0.71 (Meylan and Howard, 1995) and
- Henry's partition coefficient is calculated to H = 0.00892 atm-m^3/mole at 25 °C (corresponding to 184 kg/kg air per kg/kg water) (Meylan and Howard, 1991).

2 http://esc.syrres.com/interkow/webprop.exe?CAS=75-44-5 downloaded the 25.04.2000

9.3 Toxicological effects of phosgene

Contact with liquid phosgene can cause severe skin and eye irritation and burns with permanent damage. Inhaling phosgene can irritate the nose and throat. Further it can irritate the lungs causing coughing and /or shortness of breath. Slightly higher exposures can cause pulmonary oedema. For rats the level of phosgene giving irritation is found to be close to the levels giving lethal effects (Arts et al., 2000). Long-term effects of phosgene may be caused by repeated exposures to very low levels that can cause permanent lung damage in form of emphysema and bronchitis. Sciuto reports evidences that the lining or surfactant layer is extremely vulnerable to the toxic effects of phosgene, and thus inhibits proper alveolar gas exchange. Phosgene might also render the air/blood barrier, and evidence is shown that phosgene might penetrate the air/blood barrier and cause toxic effects in the blood (Scuito, 1998). Phosgene reacts with the NH_2-, OH- and SH- groups contained in that barrier (Schneider and Diller).

9.4 Chemical reactions of phosgene

Mertens et al. (1994) provided kinetic data for the reaction of in situ prepared phosgene using CCl_4 water mixtures irradiated by fast electrons. The hydrolysis was measured as a function of temperature and pH. This is shown in Figure 9.1. The authors found good agreement of their measurements with one other study using a very different method. The temperature dependency of hydrolysis is pronounced and the decay half-life in water at 37 ° C is t½=0.042 s corresponding with a first order decay rate of k=16.4 s^{-1}. The effect of the pOH on the hydrolysis is found negligible at about neutral pH values by the authors (Mertens et.al, 1994). For the reaction of water vapour with gaseous phosgene in air a second order rate constant is found with k = 1.2 10^{-23} $cm^3 molecule^{-1}$ s^{-1} (upper limit) at 296 K by Hatakeyama and Leu, 1989.

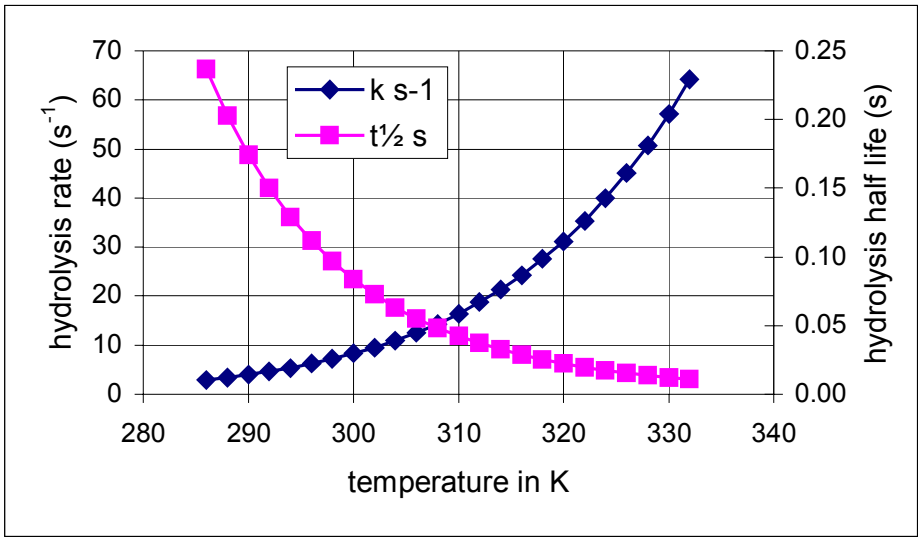

Figure 9.1. Hydrolysis of Phosgene as a function of temperature in water at pH 7

It is also found (Schneider and Diller) that phosgene reacts rapidly with amines, alcohols, and thio-alcohols, as shown in, Figure 9.2, but no rate constants could be found in the literature. Therefore, the three reactions have been lumped into one reaction assuming first order kinetics and the reaction rate is assumed to be the same as for the hydrolysis of phosgene in water.

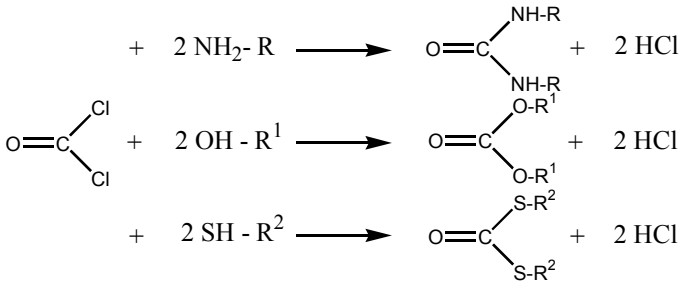

Figure 9.2. Phosgene reactions occuring in the blood-air barrier (Schneider and Diller)

9.5 A compartment model for phosgene degradation in the lung

A crude model of phosgene diffusion and reaction in the alveolar region of the lung is developed in the following. It assumes five compartments, one for the air phase and four for the lung membrane: the lining, epithelium, tissue and blood capillaries. The volumes of these compartments were calculated according to Table 9.3. For this model it is assumed that the tissue has the same volume as the blood capillaries compartment, while the overall lung model assumes only the tissue, which is filled 100% with the blood capillaries in that lung region. As the phosgene model is mainly intended for demonstration and qualitative comparison this difference will not change the main findings. The air containing part is identical with the compartment [0] in the following. The lining, epithelium, tissue and blood capillaries are regarded as compartments labelled [1] to [4], respectively.

In the lung mass exchange is assumed only between the directly connected compartments, thus between compartment [0] (air) and [1] (lining consisting mainly from water) the dimension less partition coefficient λ_{AW} is applied:

$$\lambda_{AW}=H/RT = C_{[0]}/C_{[1]} = k_1/k_0$$

H is the Henry constant, $C_{[n]}$ is the concentration of the gas in the compartment n with the volume V_n. Using a kinetic approach the equilibrium constant $\lambda_{0\ 1}$ equals k_1/k_0, with k the first order rate constants for the changes of concentration versus time. For instance, changes of compound A with the concentration C in compartment 1 is described by the differential approach:

$$d[C_{1,A}]/dt = -k_1[C_{1,A}] + k_2[C_{2,A}].$$

In case of equilibrium the number of molecules diffusing from either sides are exactly the same, thus $d[C_{1,A}]/dt = 0$. From that one receives

$$C_{1,A}/C_{2,A} = k_2/k_1 = \lambda_{12},$$

which is here described by the octanol water partition coefficient λ_{OW}. This assignment is likely to be a rough estimate only, as the epithelium also contains substantial amounts of water, which is likely to alter the equilibrium concentrations between the two layers. But as no other data are found the octanol water partition coefficient is used. For the equilibrium between the compartments [2]

and [3] and [3] and [4] an arbitrary partition coefficient of λ=1 was applied assuming that the epithelium, tissue and blood have very similar properties.

Thus the set of the equilibrium coefficients provide the ratios of the rate constants k_n. Therefore, it is sufficient to know just one rate constant to scale the model to the right dimension in time. The rate constant times the concentration is describing a mass flux that is entirely due to diffusion:

$$\frac{dm_1}{V_1 dt} = -k_1 C_1 = -\frac{DA}{\Delta x V_1}\Delta C$$

comparing both sides of the equation the rate constant is equal to:

$$k_1 = \frac{DA}{\Delta x V_1} = \frac{DA}{\Delta x V_{total}}\frac{1}{f_1} = k_{basis}\frac{1}{f_1}$$

From this the rate constants can be calculated knowing the diffusion-related parameters. The definition of $f_n = V_n/V_{total}$ is described in the next paragraph. In this model another approach was used, as a k_{basis} was calculated using time scales found in the lung model calculations: $k_{basis} = \ln 2/t$. The diffusion time for sulphur dioxide in the lining (compartment 1) was used as the characteristic time scale, giving $k_{basis}=10\ s^{-1}$.

The compartment approach results in a set of ordinary differential equations, as they are listed in Table 9.2. These equations are solved using the CHEMSIMUL program (Kirkegaard et.al, 1992, 1999). A closed system made up by a total volume is assumed in the calculation. To ease the calculations and to allow for easy scaling to calculate for other regions of the lungs the concentrations C_n are redefined. Instead a concentration X_n is defined as the mass in the total lung volume V_{total}: $X_1=m_1/V_{total}$. V_{total} is the sum of the volumes of the five compartments. Thus to calculate the concentration X_i in any compartment the following equation can be applied:

$$X_{total} = m_{total}/V_{total} = (m_0 + m_1 + m_2 + m_3 + m_4)/V_{total}.$$

Multipling each term with the corresponding V_n/V_n and defining $f_n = V_n/V_{total}$ results in :

$$X_{total} = f_0 * C_0 + f_1 * C_1 + f_2 * C_2 + f_3 * C_3 + f_4 * C_4.$$

The fraction f_n is here defined as the volume fraction of a compartment within a volume of the lung and C is the concentration in a unit volume of the respective compartment.

For the partition λ follows: $\lambda^*_{OW} = \frac{X_2}{X_1} = \frac{f_2 C_2}{f_1 C_1} = \frac{k_1/f_1}{k_2/f_2}$

This equation allows to scale the partition coefficients λ for different compartment volumes by use of the volume fractions f_n .

As input for the gas phase reaction also a water concentration is needed. Here the vapour pressure of water (relative humidity =100%) at 37 °C is used in the model giving a water partial pressure of about 6% in the lungs air.

In the following the reactions are listed in Table 9.1. This base set of rate constants are scaled on the effective diffusion in the lining RE1 and this was assumed to be of $k=10\ s^{-1}$ or $t_{½}=0.07$ s, which is the characteristic time scale for SO_2 diffusion through the lining as it is found with the other calculations. The

volume fractions are calculated according to Table 9.3 and have been included into the rate constants for the model. This is shown in Table 9.1 and in Table 9.2 the differential equation system is shown.

Table 9.1. Reaction scheme and first and second order rate constants k. The rate for RE2 and RE3 was scaled to the characteristic tome scale for SO_2 calculated by the lung model. The other rates describing diffusion are calculated from this and the respective partition coefficient λ. The values for liquid and gaseous water reactions are found in the literature and the reactions RE21 to RE24 represent the air -blood barrier reactions of phosgene assuming the same rate as for hydrolysis of phosgene.

RE1	COCl2[0]=COCl2[1]	k = 27.4	Diffusion
RE2	COCl2[1]=COCl2[0]	k = 10	
RE3	COCl2[1]=COCl2[2]	k = 10	
RE4	COCl2[2]=COCl2[1]	k = 51.3	
RE5	COCl2[2]=COCl2[3]	k = 51.3	
RE6	COCl2[3]=COCl2[2]	k = 51.3	
RE7	COCl2[3]=COCl2[4]	k = 51.3	
RE8	COCl2[4]=COCl2[3]	k = 51.3	
RE10	COCl2[0]+H2O[0]=CO2[0]+2*HCl[0]	$k_{2.order}$ = 1.2E-23	Gaseous and liquid hydrolysis
RE11	COCl2[1]=CO2[1]+2*HCl[1]	k = 16.4	
RE12	COCl2[2]=CO2[2]+2*HCl[2]	k = 16.4	
RE13	COCl2[3]=CO2[3]+2*HCl[3]	k = 16.4	
RE14	COCl2[4]=CO2[4]+2*HCl[4]	k = 16.4	
RE21	COCl2[1]=PRO[1]	k = 16.4	Air-blood barrier reactions
RE22	COCl2[2]=PRO[2]	k = 16.4	
RE23	COCl2[3]=PRO[3]	k = 16.4	
RE24	COCl2[4]=PRO[4]	k = 16.4	

Table 9.2. Differential equation system according to Table 9.1 generated by CHEMSIMUL

D[COCl2[0]]/DT	=	- K1*COCl2[0] + K2*COCl2[1] - K10*COCl2[0]*H2O[0]
D[COCl2[1]]/DT	=	K1*COCl2[0] - K2*COCl2[1] - K3*COCl2[1] + K4*COCl2[2] - K11*COCl2[1] - K21*COCl2[1]
D[COCl2[2]]/DT	=	K3*COCl2[1] - K4*COCl2[2] - K5*COCl2[2] + K6*COCl2[3] - K12*COCl2[2] - K22*COCl2[2]
D[COCl2[3]]/DT	=	K5*COCl2[2] - K6*COCl2[3] - K7*COCl2[3] + K8*COCl2[4] - K13*COCl2[3] - K23*COCl2[3]
D[COCl2[4]]/DT	=	K7*COCl2[3] - K8*COCl2[4] - K14*COCl2[4] - K24*COCl2[4]
D[H2O[0]]/DT	=	- K10*COCl2[0]*H2O[0]
D[CO2[0]]/DT	=	K10*COCl2[0]*H2O[0]
D[HCl[0]]/DT	=	2*K10*COCl2[0]*H2O[0]
D[CO2[1]]/DT	=	K11*COCl2[1]
D[HCl[1]]/DT	=	2*K11*COCl2[1]
D[CO2[2]]/DT	=	K12*COCl2[2]
D[HCl[2]]/DT	=	2*K12*COCl2[2]
D[CO2[3]]/DT	=	K13*COCl2[3]
D[HCl[3]]/DT	=	2*K13*COCl2[3]
D[CO2[4]]/DT	=	K14*COCl2[4]
D[HCl[4]]/DT	=	2*K14*COCl2[4]
D[PRO[1]]/DT	=	K21*COCl2[1]
D[PRO[2]]/DT	=	K22*COCl2[2]
D[PRO[3]]/DT	=	K23*COCl2[3]
D[PRO[4]]/DT	=	K24*COCl2[4]

Table 9.3. Characteristic morphological lung data and equilibrium constants, as well as calculated volume fractions

Values used to model the alveolar region of the lung		
Surface	108.8	m^2
V_0	$2.48 \cdot 10^{-3}$	m^3
K_{AW}	0.365	
K_{OW}	0.195	

Values for layer thicknes (m). The sum h_3+h_4 give the tissue layer thickness. In the alveoli region of the lung the tissue is filled up with blood capillaries.

alveoli:	h_1	h_2	h_3	h_4
	$5.0*10^{-8}$	$7.5*10^{-7}$	$7.5*10^{-7}$	$7.5*10^{-7}$

Volumes in m^3 calculated from the total surface area and the thicknesses except V_0

V_0	V_1	V_2	V_3	V_4	V_{total}
$2.48*10^{-3}$	$5.44*10^{-6}$	$8.16*10^{-5}$	$8.16*10^{-5}$	$8.16*10^{-5}$	$2.73*10^{-3}$

Volume fractions used in the model

f_0	f_1	f_2	f_3	f_4	f_{total}
0.908	0.002	0.03	0.03	0.03	1

9.6 Results

Using the model the time constants for formation and degradation of phosgene in the lung are found as presented in Table 9.4. It is seen that the concentrations are decreasing and only about 1.4% of the phosgene will be found in compartment 4 (blood). Also the short time delay between the compartments can be seen. The response of the model is found to be linear in concentration, thus increasing the initial concentration by e.g. a factor of 100 still 1.4 % will be found and the decay times are constant.

Table 9.4. Calculated maximum concentrations and time constants for half life for phosgene.

Compartment	Maximum concentration[3].	Time for maximum concentration (s)	Formation half life (s)	Decay half life (s)
0 Air	1.0000E+12	0	None	4.0169E-01
1 Lining	5.1608E+09	3.3397E-02	1.6698E-02	4.2942E-01
2 Epithelium	1.4331E+10	3.3397E-02	1.6698E-02	4.2947E-01
3 Tissue	1.3832E+10	3.3397E-02	1.6698E-02	4.2951E-01
4 Blood	1.3584E+10	3.3397E-02	1.6698E-02	4.2953E-01

In Figure 9.3 the equilibrium for phosgene in the lung compartments have been calculated only using the equations RE1 to RE8. Here it can be seen that the equilibrium is achieved within tenth of seconds. The concentration of compartment [0] decreases only slightly, due to its large volume fraction, while the con-

3 The concentrations are given as m_n/V_{total} in molecules/cm^3 : 1e12 molecules/cm^3 is about 0.04 ppm in the gas phase

centration of phosgene in compartment [1] is the highest. The ratio of the concentrations resembles the respective partition coefficient.

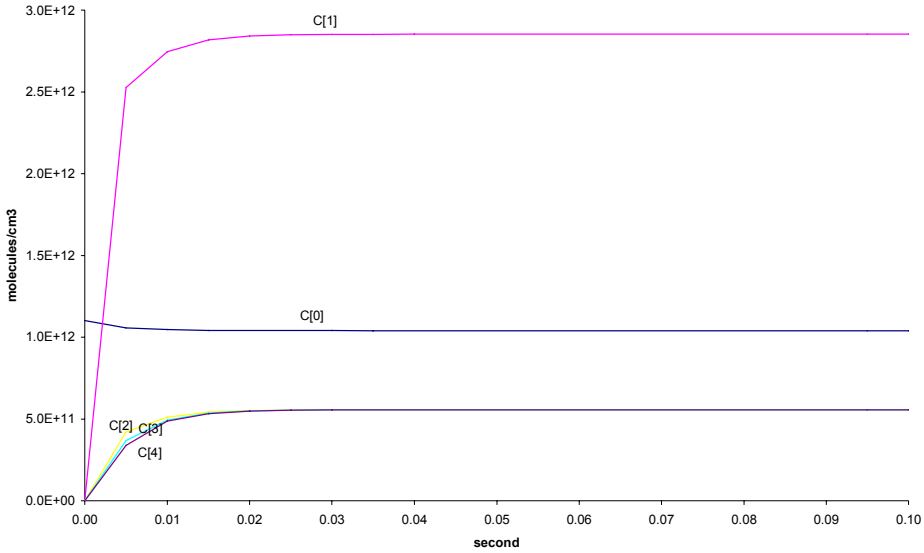

Figure 9.3. Simulation of the phosgene distribution in the lung without chemical reactions

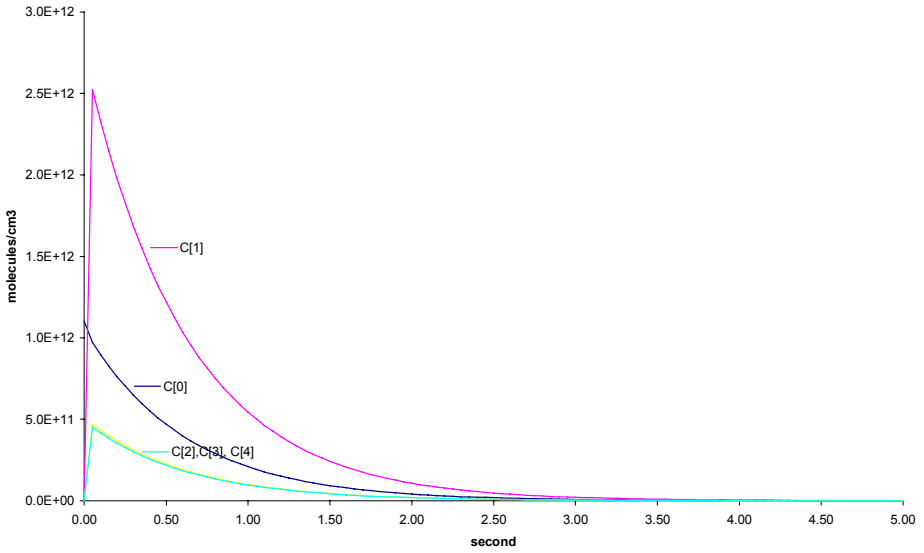

Figure 9.4. Simulation of the phosgene distribution in the lung including chemical reactions

In Figure 9.4 also the degradation reactions have been modelled and it can be seen that all the phosgene will be degraded within 2 to 3 s which would be within one single inhalation cycle. This might be an upper limit for the degradation of phosgene in the lung, as this compartment model does not include phosgene convection in the lung and blood perfusion through the lung. There will be the products HCl, CO_2 and unspecified products PRO (i.e. products from reaction with amino acids) in the lung after reaction. As the rate constants for the formation of these products are set to the same value, it is sufficient to discuss the behaviour of HCl as it will be fully representative for the other products too. The only difference is that PRO is not included within compartment 0. The HCl

results are shown in Figure 9.5. It can be seen that the concentrations in the different compartments are very different and that the concentration in compartment 1 is the highest, while it is by far lowest for the compartment 0. In Table 9.5 the distribution of HCl based on the volume of the total lung is shown. It can be seen that the HCl yield in the compartment 0 is almost negligible, thus the hydrolysis is most relevant in the compartments containing water.

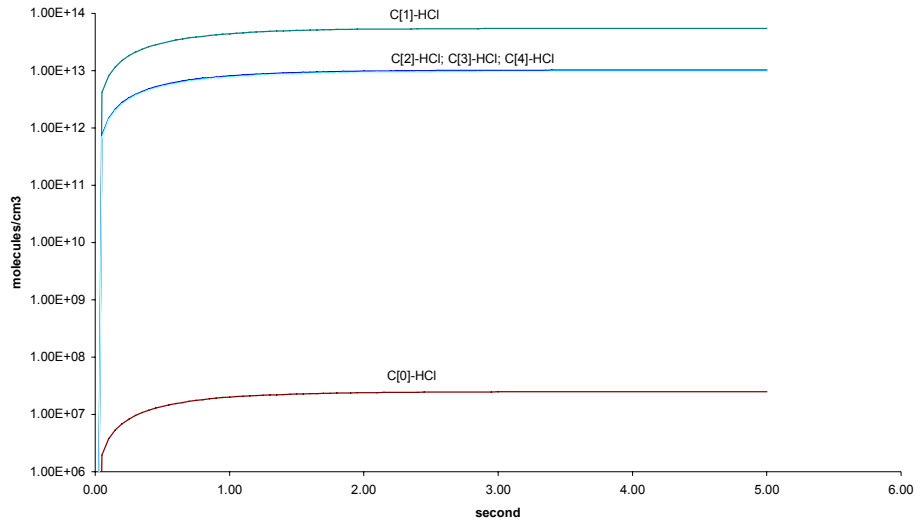

Figure 9.5. Formation of hydrogen chloride

Table 9.5. The maximum concentrations C_n for HCl (based on the total lung volume) and the distribution in percent. Theoretically 2.00E+12 molecules of HCl could be produced, but here 50% of the phosgene is degraded through reaction: COCl2[n] →PRO[n].

HCl max values	C_0	C_1	C_2	C_3	C_4	C_{total}
molecules/cm^3	2.27E+07	1.10E+11	3.06E+11	2.95E+11	2.89E+11	1.00E+12
% of total HCl	0.002	11.0	30.6	29.5	28.9	100.0

9.7 Discussion

In this chapter a crude model for phosgene distribution and degradation in the lung is developed. Only very few rate constants have been found in the literature directly, others have been calculated using relevant equilibrium constants and an assumed characteristic time scale for the lining which is within the diffusion time scales for the other gases found by modelling them with the lung model. The lung compartment volumes have been calculated from the overall surface area and the cell diameters for the alveoli region given elsewhere in this report. From that volume fractions f_n have been calculated used to scale the basis rate constants k to the appropriate lung dimensions. By doing so the partition coefficients are maintained.

Due to the lack of experimental data the findings of phosgene degradation and HCl formation can only be described qualitatively. The most remarkable finding is the high concentration of phosgene and HCl in the lining, which is in agreement with the pathological findings. Also the fact that the phosgene is hydrolysed mainly in the lungs tissue is in agreement with the literature. In this model

regardless the initial phosgene concentration a fraction of phosgene will be found in the blood capillary compartment. This might be in contradiction with the toxicological findings, that only rather high concentrations of phosgene are likely to diffuse into the blood capillaries. The reason for this could be an underestimation of the reaction rates describing the air blood barrier, which is based on an assumption only.

This procedure will be applicable for other gases and also for other parts of the lung or different segments. This type of modelling will support the establishment and understanding of experiments and modelling of penetration of lung probes/tissue with gases. It also supports the prediction of rate constants not directly measurable. Rate constants established and verified by this experimental/theoretical approach can easily be included into the lung model described in chapter 1 - 6. Knowing more about the reaction mechanisms and the biochemical response, more complex reaction systems can be established. This will be important to better predict time delayed effects as oedema formation.

10 Conclusions

10.1 Results from this study

This report provides a description of a mathematical model to predict the internal concentrations (the internal exposure) within elements of the respiratory system in response to external exposures to toxic substances. The model has a high degree of detail, discriminating more than 30 elements in the human respiratory system, each divided into an air volume, lining, epithelium and supporting tissue, the latter being perfused with blood.

The model accounts for turbulent and laminar convection of air through the elements during each respiration cycle, lateral molecular diffusion in the air phase, and transverse molecular diffusion through the wall layers (lining, epithelium and tissue)

The information about the overall geometry of elements in the respiratory system of humans and rats is rather complete. There is however limited information about the dimensions of wall layers (thickness of lining, epithelium and supporting tissue), so part of the information provided (and applied) in this report is based on inter- and extrapolations, and subjective interpretations of microscopic photographs.

The model has been validated using published experiments involving diethylether and acetone. Results for diethylether, which is a slightly soluble substance, are good, in case of acetone, a very soluble substance, differences occur for which no full explanation exists as by now. Comparisons with experiments on chlorine are hard to interpret because of the reactivity of chlorine.

Improvements of the model for soluble substances may be obtained using better descriptions of the wall compartments; better data on solubility and diffusivity in the wall compartments; better information on mass transport in the nasal/oral regions; or including chemical reactions.

Using the model, time scales and internal exposure concentrations have been calculated for a number of substances (ammonia, sulphur-dioxide and hydrogen-sulphide), both for the human respiratory system as well for the respiratory system of a rat.

Both time scales and exposure concentrations depend on the solubility of the substances. For very soluble substances (ammonia, hydrochloric acid, acetone) the time scales are largest, for humans in the order of a few to 20 seconds for

lining and epithelium, the longer time scales occurring in the deeper parts of the lung. Time scales for tissue in the nasal/oral region is in the order of one to several minutes. In humans, internal exposure concentrations seem to be rather uniform (about 80% of the external concentration) down to the terminal bronchioles, and reduced to almost zero at the first alveolar ducts.

In rats time scales are larger due to more effective absorption, probably at the larger surface area in the nasal passages, also causing less penetration of the substance in the upper airways. During the calculations, concentrations at the trachea were already reduced to about 25%.

The difference of internal exposure in humans and rats for very soluble gases should be noted, as they are quite opposite (as regards to time scales) from a-priori expectations.

For less soluble substances, time scales in humans are extremely short. Within one or two inhalations, equilibrium conditions throughout the respiratory system are reached, the only exception being the tissue in the nasal/oral region. Internal concentrations are close to the external concentrations down to the terminal bronchiole. Depending on the solubility, the substances penetrate deeper into the alveolated parts of the lung. For sulphur-dioxide, with an average alveolar concentration of 10% of the exposure concentration, the penetration is limited. For hydrogen-sulphide (average alveolar concentration 50%), the substance has a uniform concentration throughout the alveolar region.

For these less soluble substances (sulphur-dioxide), the difference between humans and rats are less than for ammonia, though effects of absorption in the upper airways are still more pronounced compared to humans. Time scales are (in absolute terms) comparable to humans, i.e. a few seconds for lining and epithelium.

The information is used to provide a method to predict the internal exposure in response to exposure to fluctuating concentrations.

Considering the short time scales that appeared in this study, one can conclude that attention should be paid to both effects of as well as prediction of fluctuating concentrations up to frequencies of 0.1-0.2 Hz for substances that cause local damage to the respiratory system.

We have been unable to derive guidelines how to apply concentration-time-fatality relations (Probit functions) to fluctuating concentration time series. The concentration-time-fatality relations are based on exposure to constant concentrations over 5 minutes. These relations can probably be extrapolated to an exposure over about 1 minute. But it is uncertain how these relations should be applied to fluctuations at smaller time scales. We demonstrated that considerable difference occur in predicted fatality rates, if real fluctuating concentration data is processed either by extrapolating the concentration-time-fatality relations to the relevant exposure frequencies (0.1 Hz) or by taking 1-minute maximum concentrations.

As an example of modelling chemical reactions in lung tissue, we concentrated on phosgene. Results are in agreement with literature. This type of modelling can support dedicated experiments, e.g. in-vitro experiments, looking at absorption of substances in tissue and the damage to tissue caused by these substances.

10.2 Recommendations

A critical element in the performance of the model appeared to be the diffusion of substances in cell tissue. Assessment of diffusion rates in cell tissue as compared to continuum aqueous phases would improve the reliability of the model.

Likewise, solubility of substances needs attention, especially for reactive substances, where solution in the aqueous phase is accompanied by chemical transformation. Acidity and presence of other substances can be important factors, reason why data from solubility in pure water may not be sufficient, and chemical reactions in the wall compartments may be important to predict the correct absorption of the substance in the airways.

This study only considered the internal exposure concentrations with respect to levels and time scales. No progress was made regarding understanding the processes that cause damage and the time scales related to these processes. This is a necessary prerequisite in order to be able to link existing knowledge on toxicity of substances to exposure to fluctuating concentrations.

The preliminary recommendation from the parallel study (Arts et al., 2000) to use maximum concentrations over 1 minute for short duration exposures in combination with the conclusion from this study mean, that atmospheric dispersion models need to provide information about concentration fluctuations down to time scales of 5 to 10 sec.

References

Arts, J.H.E., Mommers, C., Muijser, H., 2000, *Toxic effects from accidental releases of hazardous substances (TEARHS) – Lethal and non-lethal effects in rats upon exposure during short periods of time*, TNO Nutrition and Food Research, Zeist, The Netherlands, TNO report V99.1136

Handbook of Chemistry and Physics, 80th ed. D.R. Lide et al., CRC Press London, 1999

Fiserova-Bergova, F., 1983, Gases and their solubility: a review of fundamentals, in: Fiserova-Bergova, F., (ed.) *Modeling of Inhalation Exposure to Vapors*, Vol. I, CRC Press, Inc, Boca Raton, Florida.

Gargas, M.L., Medinsky, M.A., Andersen, M.E., 1993, Advances in Physiological Modeling Approaches for Understanding the Disposition of Inhaled Vapors, in: D.E. Gardner, J. D. Crapo, R.O. McClellan (eds.), *Toxicology of the Lung*, 2nd Ed., Target Organ Toxicology Series, Raven Press New York.

Gehr P., Geiser M., Stone K.C., Crapo J.D., 1993 Morphometric Analysis of the Gas Exchange Region of the Lung, in: D.E. Gardner, J. D. Crapo, R.O. McClellan (eds.), *Toxicology of the Lung*, 2nd Ed., Target Organ Toxicology Series, Raven Press New York

Guilmette, R.A., Wicks, J.D., Wolff, R.K., 1989, Morphometry of human nasal airways *in vivo* using magnetic resonance imaging, J. of Aerosol Medicine, Vol. 2 No. 4.

Handbook of Chemistry and Physics, 1999, 80th ed., D.R. Lide et al. eds, CRC Press London,

Hardy, Edagar E., Phosgene, in Kirk-Othmer *Encyclopedia of chemical technology*, 3rd edition, vol. 17, 416 - 425

Hatakeyama, Shiro and Leu, Ming-Taun, *Rate constants for reactions between atmospheric reservoir species 2. H_2O*, J.Phys. Chem. (1989) 93 5784

Hoppin, F.G., Hildebrandt, J., 1977, Mechanical Properties of the Lung, in West, J.B. (ed.) *Bioengineering Aspects of the Lung,*Marcel Dekker, Inc., New York.

Horsfield, K., Kemp, W., Phillips, S., 1982, An asymmetrical model of the airways of the dog lung, , J. Appl. Physiol. Vol. 52 pp 21-26.

ICRP, 1994, Human respiratory tract model for radiological protection Annals of the ICRP, Vol. 24, 1-3 (ICRP Publication 66).

Johanson, G. 1991, Modelling of respiratory exchange of polar solvents, Ann. occup. Hyg. Vol. 35 No 3 pp 323-339.

Kirkegaard, P.; Bjergbakke, E., 1999, *CHEMSIMUL: A simulator for chemical kinetics*. Report Risø-R-1085 (1999,revised 2000)

Kirkegaard, P. ,Rasmussen, O.L.; Bjergbakke, E. ; Pagsberg, P..1992; *CHEMSIMUL - software and methods for numerical simulation of chemical reaction systems.* Industrial Mathematics Week, Trondheim August 1992, Proceedings, p.174 - 181

Landolt-Börnstein, 1962, Zahlenwerte und funktionen aus Physik-Chemie-Astronomie-Geophysik und Technik, 6. Edition, Vol. II/2b, Lösungsgleichgewichte I, Springer Verlag, Berlin

Landolt-Börnstein, 1969, Zahlenwerte und funktionen aus Physik-Chemie-Astronomie-Geophysik und Technik, 6. Edition, Vol. II/5a, Transportphänomene I, Springer Verlag, Berlin

Linke, W.F., Seidell, A., (eds.) 1958, Solubilities - Inorganic and metal-organic compounds, Volume I, 4th ed. D. Van Nostrand Compant, Inc., Princeton, New Jersey

Menzel, D.B., Amdur, M.O., 1986, Toxic Responses of the Respiratory System, Chapter 12 in: C.D. Klaassen, M.O. Amdur and J. Doul (eds.) *Casarett and Doull's Toxicology - The Basic Science Of Poisons*, 3rd ed. Macmillan Publishing Company, New York.

Mertens, Ralf; von Sonntag, Clemens, Lind, Johan and Merenyi, Gabor, *A kinetic study of the hydrolysis of phosgene in aqueous solution by pulse radiolysis*, Angew. Chem. Int. Ed. Engl. (1994) 33 no 12 1259

Meylan,W.M. and P.H. Howard. 1991. *Bond contribution method for estimating Henry's law constants.* Environ. Toxicol. Chem. 10:1283-1293

Meylan, W.M. and P.H. Howard. 1995, *Atom/fragment contribution method for estimating octanol-water partition coefficients.* J. Pharm. Sci. 84:83-92.

Miller, F.J., Overton, J.H.,Jaskot, R.H., Menzel, D.B., 1985, A model of the regional uptake of gaseous pollutants in the lung, I. The sensitivity of the uptake of ozone in the human lung to lower respiratory tract secretions and exercise, Toxicology and applied pharmacology, Vol. 79, pp. 11-27.

Miller, F.J., Overton, J.H., Kimbell, J.S., Russell M.L., 1993, Regional Respiratory Tract Absorption of Inhaled Reactive Gases, in: D.E. Gardner, J. D. Crapo, R.O. McClellan (eds.), *Toxicology of the Lung*, 2nd Ed., Target Organ Toxicology Series, Raven Press New York. pp. 485-526

Morris, J.B., Hassett, D.N., Blanchard, K.T.A., 1993, Physiologically Based Pharmacokinetic Model for Nasal Uptake and Metabolism of Nonreactive Vapors, Toxicology And Applied Pharmacology 123, pp. 120-129

Nielsen, M., Ott, S., 1995, *A Collection of Data from Dense Gas Experiments*, Risø National Laboratory, Roskilde, Denmark, Risø-R-845(EN)

Nielsen, M., Ott, S., 1996, *Fladis Field Experiments Final Report*, Risø National Laboratory, Roskilde, Denmark, Risø-R-898(EN)

Nodelman, V., Ultman, J.S., 1999, Longitudinal distribution of chlorine absorption in human airways: comparison of nasal and oral quiet breathing, J. Appl. Physiol. 86 (6), pp 1984-1993.

Nunn, J.F., 1993, *Nunn's Applied Respiratory Physiology*, 4th ed., Butterworth-Heinemann Ltd, Oxford.

Podgórsky, A., Gradón, L., 1993, An improved mathematical model of hydrodynamical self-cleansing of pulmonary alveoli, Ann. ocup. Hyg., Vol 37 No 4, pp. 347-365

Roth-Weller, 1999, *Gefährliche Chemische Reaktionen*, edition 7/99, ecomed verlagsgesellschaft AG &Co. KG

Schneider, Wolfgang ; Diller Werner, *Phosgene*, in Ullmann's Encyclopedia of Industrial Chemistry, 5th edition, Vol. A 19 page 411-420

Schreider, J.P., Raabe, O.G., 1981, Anatomy of the Nasal-Pharyngeal Airway of Experimental Animals, Anat. Rec. Vol. 200 pp. 195-205.

Schrikker, A.C.M., Vries, W.R. de, Zwart, A., Luijendijk, S.C.M., 1985, Uptake of highly soluble gases in the epithelium of the conducting airways, Pflügers Arch. Vol. 405 pp 389-394.

Scuito, Alfred M., 1998, *Assessment of early acute lung injury in rodents exposed to phosgene,* Arch. Toxicol. , 78, 283-288

Silvermand, L., Whittenberger, J.L., Muller, J., 1949, Physiological response of man to ammonia in low concentrations, Journal of industrial hygiene and toxicology, Vol. 31, no 2, pp 74-78

St.George, J.A., Harkema, J.R., Hyde, D.M., Plopper, C.G., 1993, Cell Populations and Structure/Function Relationships of Cells in the Airways, in: D.E. Gardner, J. D. Crapo, R.O. McClellan (eds.), *Toxicology of the Lung*, 2nd Ed., Target Organ Toxicology Series, Raven Press New York.

Tennekes, H. Lumley, J.L., 1974, *A First Course In Turbulence*, The MIT Press, Cambridge, England, 3rd-6th printing.

Thorpe, C.W., Bates, J.H.T., 1997, Effect of stochastic heterogeneity on lung impedance during acute bronchoconstriction: a model analysis, J. Appl. Physiol. Vol. 82 No. 5 pp 1616-1625.

Weibel, E.R., 1963, *Morphometry of the Human Lung*, Springer Verlag, Berlin.

Weibel, E.R., Gil, J., 1977, Structure-function relationships at the alveolar level, in West, J.B. (ed.) *Bioengineering Aspects of the Lung,*Marcel Dekker, Inc., New York.

Whitney, R.P., Vivian, J.E., 1941, Solubility of Chlorine in water, Industrial and Engineering Chemistry Vol. 33 No 6, pp 741-744.

Yeh, H.C., Schum, G.M., Duggan, M.T., 1979, Anatomic Models of the Tracheobronchial and Pulmonary Regions of the Rat, Anat. Rec. Vol. 195, pp 483-492.

Åstrand, I., 1983, Effect of physical exercise on uptake, distribution and elimination of vapors in man, in: Fiserova-Bergerova, V., (ed.) *Modeling of inhalation exposure to vapors*, Vol. II, pp 107-130, CRC Press, Boca Raton, Florida.

Bibliographic Data Sheet **Risø-R-1208(EN)**

Title and authors

TEARHS - Modelling toxic impacts on the airway system from exposure to fluctuating concentrations

Nijs Jan Duijm, Frank Markert, Søren Ott

ISBN	ISSN
87-550-2750-4 87-550-2751-2 (Internet)	0106-2840

Department or group	Date
System Analysis Department	August 2000

Groups own reg. number(s)	Project/contract No(s)
SYS-231-47, PSP 1210301	ENV4-CT97-0628

Pages	Tables	Illustrations	References
63	24	27	44

Abstract (max. 2000 characters)

This report describes Risøs contribution to the TEARHS project. The aim of the TEAHRS project is to develop and assess methodologies to determine the acute toxicity of inhalation of fluctuating concentrations of hazardous substances as a contribution to the improvement of quantitative risk assessment.

A mathematical model is described that predicts the physical and chemical processes in the airways during short exposures to toxic substances. Based on this modelling, it has been assessed how fast and to what level tissue in the airways is exposed to the substance. These time scales turn out to be small, in the order of a few seconds. Considering the aspiration pattern, it is concluded that relevant time scale for absorption in the airways is 5 to 10 seconds. In real atmospheric, toxic gas clouds, fluctuations at this time scale are large. There is still a large gap between the empirical information on toxic effects and the relevant time scale for exposure. Concentration-time-fatality relations are obtained from experiments with rats down to 5 minutes of exposure. If the information from these relations is extrapolated down to 5 to 10 seconds using different assumptions, the predicted mortality is quite different.

This study indicates that atmospheric dispersion models for acutely toxic substances need to provide information about concentration fluctuations of time scales of 5 to 10 sec. Final conclusions can only be drawn when it becomes clear how the gap between concentration-time-fatality relations and short duration fluctuations can be closed.

Descriptors

TOXICITY; TOXIC GASES; EXPOSURE; RESPIRATORY SYSTEM; LUNGS; CONCENTRATIONS; FLUCTUATIONS; MODELS; AMMONIA; CHLORINE; HYDROCHLORIC ACID; HYDROGEN SULPHIDE; PHOSGENE; SULPHUR DIOXIDE

Available on request from Information Service Department, Risø National Laboratory,
(Afdelingen for Informationsservice, Forskningscenter Risø), P.O.Box 49, DK-4000 Roskilde, Denmark.
Telephone +45 4677 4004, Telefax +45 4677 4013